Dynamical Downscaling–Based Projections of Great Lakes Water Levels*,+

MICHAEL NOTARO AND VAL BENNINGTON

Nelson Institute Center for Climatic Research, University of Wisconsin–Madison, Madison, Wisconsin

BRENT LOFGREN

NOAA/Great Lakes Environmental Research Laboratory, Ann Arbor, Michigan

(Manuscript received 11 December 2014, in final form 9 July 2015)

ABSTRACT

Projections of regional climate, net basin supply (NBS), and water levels are developed for the mid- and late twenty-first century across the Laurentian Great Lakes basin. Two state-of-the-art global climate models (GCMs) are dynamically downscaled using a regional climate model (RCM) interactively coupled to a one-dimensional lake model, and then a hydrologic routing model is forced with time series of perturbed NBS. The dynamical downscaling and coupling with a lake model to represent the Great Lakes create added value beyond the parent GCM in terms of simulated seasonal cycles of temperature, precipitation, and surface fluxes. However, limitations related to this rudimentary treatment of the Great Lakes result in warm summer biases in lake temperatures, excessive ice cover, and an abnormally early peak in lake evaporation. While the downscaling of both GCMs led to consistent projections of increases in annual air temperature, precipitation, and all NBS components (overlake precipitation, basinwide runoff, and lake evaporation), the resulting projected water level trends are opposite in sign. Clearly, it is not sufficient to correctly simulate the signs of the projected change in each NBS component; one must also account for their relative magnitudes. The potential risk of more frequent episodes of lake levels below the low water datum, a critical shipping threshold, is explored.

1. Introduction

The Laurentian Great Lakes contain Earth's largest surface freshwater resources, support a vast population within their watersheds, and are vital to the U.S. and Canadian economies. Their basin has been a regional hotspot in observed climate change, including rising air temperatures, reduced cloud cover, more frequent heavy precipitation events, rapid lake warming, and diminished lake ice cover. Annual air temperatures across the U.S. Midwest increased by at least 0.8°C during 1900–2010 (Kunkel et al. 2013; Pryor et al. 2014). The wintertime warming trend of +0.4°–0.7°C decade^{-1} during 1973–2010 across the basin led to a 71% reduction in Great Lakes ice cover (Wang et al. 2012). Declining ice cover, along with more frequent intense cyclones tracking across the basin, has supported a positive trend in lake-effect snowfall since the early twentieth century (Angel and Isard 1998; Burnett et al. 2003; Ellis and Johnson 2004; Kunkel et al. 2009). Higher air temperatures and an associated enhancement in the saturation water vapor pressure of the atmosphere have led to more frequent heavy precipitation events (Kunkel et al. 1999, 2003). Lake Superior's surface water temperatures during July–September increased by +2.5°C during 1979–2006, at a far greater rate than the regional atmospheric warming (Austin and Colman 2007). During 1985–2008, the atmospheric surface layer over Lake Superior became increasingly destabilized and overlake winds accelerated during the lake stable summer months, resulting from rising air and water temperatures and a diminished lake–atmosphere temperature gradient (Desai et al. 2009). Cloud cover decreased over the lakes by −2% decade^{-1} during 1982–2012 (Ackerman et al. 2013).

* Supplemental information related to this paper is available at the Journals Online website: http://dx.doi.org/10.1175/JCLI-D-14-00847.s1.

+ Center for Climatic Research Contribution Number 1334.

Corresponding author address: Michael Notaro, Nelson Institute Center for Climatic Research, University of Wisconsin–Madison, 1225 West Dayton St., Madison, WI 53706.
E-mail: mnotaro@wisc.edu

DOI: 10.1175/JCLI-D-14-00847.1

Anomalously mild conditions contributed to persistently low lake levels on Lakes Superior, Michigan, and Huron during 1999–2012. Clearly, the regional climate of the Great Lakes basin is rapidly changing, with direct consequences to the lakes.

The Laurentian Great Lakes are an invaluable resource to both society and regional wildlife, containing about 18% of the global freshwater supply (Botts and Krushelnicki 1988). The lakes have a total surface area of 246 000 km^2 and coastline of about 17 000 km, with over 37 million inhabitants within their watershed (Beltran et al. 1995). They impact shipping, fishing, drinking water, manufacturing, power production, wastewater treatment, and recreation, leading to 1.5 million jobs and $62 billion in wages per year (Vaccaro and Read 2011). The Great Lakes basin is rich in animal, fish, and plant biodiversity, containing at least 153 established fish species (Crossman and Cudmore 1998) and serving as a key migratory and breeding zone for millions of birds. Their wetlands provide spawning and nesting habitat for animals, limit erosion, and protect water quality. Given the importance of the Great Lakes and rapid ongoing climate change, it is necessary to develop reliable regional climate change and lake level projections for the twenty-first century to aid in risk assessments and formation of effective adaptation strategies.

Climate change and associated lake level responses will likely affect the economy (e.g., loss of shipping and hydropower, greater navigation challenges) and environmental conditions (e.g., loss of wetlands, shoreline changes) of the Great Lakes basin (Hartmann 1990). Over 200 million tons of cargo are shipped annually across the lakes (Wang et al. 2012). For every inch of reduced lake level, the cargo capacity of a 1000-foot ship is reduced by 270 tons (1 U.S. ton $\approx$ 907.1847 kg), according to the Great Lakes Carriers Association, and an estimated $11 000–$22 000 in daily shipping profits is lost per ship (Lindeberg and Albercook 2000; Wang et al. 2012). Modest lake level fluctuations can incur significant losses in lake shipping, hydroelectric power generation, and shoreline erosion (Bruce 1984; Kling et al. 2003; Wang et al. 2012). Climate change can be both beneficial and detrimental to the region's shipping industry by extending the ice-free shipping season, increasing costs, and requiring further dredging of harbors and channels and modifications of docks, water intake pipes, and additional infrastructure (Changnon 1993; Kling et al. 2003; Millerd 2011; Pryor et al. 2014). Higher air temperatures will elevate the demand for lake water withdrawal for irrigation and power plant cooling (Adams et al. 1990; Linder and Inglis 1989). Declining lake ice cover affects the regional economy (Niimi 1982), aquatic ecosystems (Vanderploeg et al. 1992; Brown et al. 1993; Magnuson et al. 1995; Kao et al. 2015), and water level variability (Assel et al. 2004). Higher water temperatures can produce lower oxygen levels and anoxia in bottom waters (Mortsch and Quinn 1996; Kling et al. 2003). Higher summer water temperatures and anoxia in the deeper waters can elevate mercury release from sediments and increase the mercury level in fish (Bodaly et al. 1993; Yediler and Jacobs 1995; Grigal 2002; Kling et al. 2003). Higher temperatures, greater precipitation, and longer growing seasons support the production of blue-green and toxic algae, which harm fish, habitats, and water quality (Reutter et al. 2011; Mackey 2012; Ficke et al. 2007; Pryor et al. 2014). Lake temperature changes can affect the health, survival, and productivity of phytoplankton, zooplankton, and fish species and the spread of invasive species (Mortsch and Quinn 1996).

Numerous modeling studies since the mid-1980s have developed projections of regional climate, net basin supply (NBS), and lake levels for the Great Lakes basin (Gronewold et al. 2013; Mallard et al. 2015) (Table 1). The water levels are determined by the three components of NBS—namely, overlake precipitation, lake evaporation, and drainage basin runoff—along with diversions in and out of the basin and channel flow between lakes. Early on, Bruce (1984) recognized the challenge of predicting lake levels, given the uncertainty of projections and relative contribution of each individual NBS component.

Despite considering a range of global climate models (GCMs) (e.g., Angel and Kunkel 2010), nearly every study of Great Lakes water level projections has applied some version of the Great Lakes Environmental Research Laboratory (GLERL) suite of models to simulate the NBS components. This suite consists of the large basin runoff model (LBRM), large lake thermodynamics model (LLTM), and coordinated Great Lakes regulation and routing model (CGLLRM). These studies in Table 1 generally forced the hydrologic model with GCM-based climate anomalies superimposed onto observed data, early on based on steady-state 2 $\times$ CO_2 simulations (Croley 1990; Hartmann 1990; Smith 1991; Mortsch and Quinn 1996) but later advancing into transient climate simulations (Chao 1999; Mortsch et al. 2000; Lofgren et al. 2002; Hayhoe et al. 2010; Angel and Kunkel 2010). The GCMs were extremely coarse, often without representation of the Great Lakes. Studies applying the GLERL suite usually predicted large lake level declines due to the following mechanism (Croley 1990; Smith 1991; Mortsch and Quinn 1996; Croley et al. 1996; Hayhoe et al. 2010). Runoff was projected to decrease and occur earlier resulting from reduced snowpack and enhanced plant transpiration in response to higher air temperatures, which dried the soil. Higher air

TABLE 1. Summary of prior studies of projected Great Lakes NBS and lake levels, including the study reference, source of climate data, horizontal resolution of the atmospheric model, emission scenario, time period for the projections, type of GCM simulations considered (steady-state 2 × CO_2 runs vs transient runs), hydrologic or hydraulic models forced with the climate projections, and resulting range of projections in NBS (%) and lake levels (m) (GL: Great Lakes, SUP: Lake Superior, MI–HUR: Lakes Michigan–Huron, ONT: Lake Ontario, and ERI: Lake Erie). The GLERL suite consists of the LBRM, LLTM, and CGLRRM. Studies applying the GLERL suite forced the hydrologic model with GCM-based mean climate anomalies superimposed onto observed time series of historical climate data.

Study	Climate data	Grid	Scenario	Projection time period	Run type	Hydrologic model	Projection NBS	Projection lake levels
Cohen (1986)	2 GCMs	6.2° lat × 8.8° lon	2 × CO_2	—	Steady state	Water balance calculations	GL: −4% to −21%	—
Marchand et al. (1988)	1 GCM	4° lat × 5° lon	2 × CO_2	—	Steady state	Great Lakes levels/flow model	—	SUP: −0.21 m and ONT: −0.85 m
Croley (1990)	3 GCMs	5.4° lat × 7.5° lon	2 × CO_2	—	Steady state	GLERL suite	SUP: −26% and ERI: −87%	—
Hartmann (1990)	3 GCMs	5.4° lat × 7.5° lon	2 × CO_2	—	Steady state	GLERL suite	SUP: −26% and ONT: −28%	SUP: −0.47 m and MI–HUR: −1.59 m
Smith (1991)	3 GCMs	5.4° lat × 7.5° lon	2 × CO_2	—	Steady state	GLERL suite	—	SUP: −0.45 m and MI–HUR: −1.58 m
Mortsch and Quinn (1996)	4 GCMs	5.0° lat × 6.6° lon	2 × CO_2	—	Steady state	GLERL suite	—	SUP: −0.39 m and MI–HUR: −1.60 m
Croley et al. (1996)	Transposed observed data	—	—	—	—	GLERL suite	GL: −1% to −54%	—
Chao (1999)	4 GCMs	4.1° lat × 5.2° lon	IPCC Second Assessment Report (AR2)	2050	Transient	GLERL suite	—	SUP: −0.5 m and MI–HUR −0.9 m
Mortsch et al. (2000)	2 GCMs	3.1° lat × 3.8° lon	+1% CO_2 yr^{-1}	2050	Transient	GLERL suite	—	SUP: −0.16 m and MI–HUR: −0.49 m
Lofgren et al. (2002)	2 GCMs	3.1° lat × 3.8° lon	+1% CO_2 yr^{-1}	2090	Transient	GLERL suite	—	SUP: −0.16 m and MI–HUR −0.52 m
Hayhoe et al. (2010)	3 CMIP3 GCMs	2.4° lat × 2.8° lon	SRES A1FI	2070–99	Transient	GLERL suite	—	SUP: −0.2 m and MI–HUR: −0.55 m
Angel and Kunkel (2010)	23 CMIP3 GCMs	2.5° lat × 2.8° lon	SRES B1, A1B, and A2	2080–94	Transient	GLERL suite	—	MI–HUR: −0.25 m for B1 to −0.41 m for A2
MacKay and Seglenieks (2013)	1 RCM	22.5 km	SRES A2	2021–50	Transient	RCM hydrologic components and CGLRRM	ERI: −9% and SUP: +1%	SUP: −0.03 m and ERI: −0.06 m
Music et al. (2015)	3 RCMs	45–50 km	SRES A2	2041–70	Transient	RCM hydrologic components	MI–HUR: +1%	—

temperatures resulted in warmer lakes, less ice cover, and greater atmospheric saturation vapor pressure, which increased lake evaporation. Reduced runoff and enhanced evaporation led to projected lower lake levels. Lofgren et al. (2011) later identified a critical issue in the treatment of evapotranspiration by the GLERL suite that explains the flawed consensus of projected lower lake level among these studies, as elaborated upon later.

Climate transposition studies (Croley et al. 1998; Kunkel et al. 1998) examined the Great Lakes' hydrologic response to projected warming, while avoiding the known limitations of GCMs, by forcing the GLERL suite with historical observed daily climate data from a range of climate zones presently located to the south of the basin. Transposed climates generally led to greater overland evapotranspiration, diminished soil moisture and runoff, reduced snowpack, warmer lakes, greater lake evaporation, and diminished NBS.

Lofgren et al. (2002) was the first to demonstrate the potential for higher lake levels, given a scenario of modest warming and substantial precipitation increases. Lofgren et al. (2011) identified a serious flaw in the treatment of overland evapotranspiration in many land surface models (LSMs), including the GLERL suite, putting the general consensus of prior studies of future declining lake levels in question. Many LSMs use air temperature as a proxy to compute potential evapotranspiration (PET) and project large increases in future evapotranspiration. This approach neglects the fundamental requirement of LSMs to maintain a balance between incoming and outgoing energy (Lofgren et al. 2011; Gronewold et al. 2013). The surface energy budget that is implied in the hydrologic model is inconsistent with that of the GCM, which is forcing the offline hydrologic model. Lofgren et al. (2011) encouraged an energy budget–based approach to computing PET, which satisfies energy conservation and leads to projections of modest declines or even increases in lake levels.

Recent studies have applied high-resolution regional climate models (RCMs) to develop twenty-first-century projections for the Great Lakes basin (Gula and Peltier 2012; MacKay and Seglenieks 2013). Gula and Peltier (2012) produced regional climate projections (without examining NBS or lake levels) by dynamically downscaling one of the GCMs from phase 3 of the Coupled Model Intercomparison Project (CMIP3); however, their methodology lacked two-way lake–atmosphere coupling. MacKay and Seglenieks (2013) developed projections of NBS and lake levels by dynamically downscaling one GCM using an RCM, debiasing the simulated NBS, and using this NBS to force a river-routing and lake level scheme. This approach improved upon traditional approaches of estimating NBS by applying higher spatial resolution; representing surface water, land surface–atmosphere feedbacks, and soil and vegetation processes; and considering changes in climate variability. The inclusion of two-way land–atmosphere coupling, which is critical to lake-effect processes and moisture recycling, led to smaller projected declines in NBS and lake levels than in prior studies. Notaro et al. (2015) applied dynamical downscaling to two GCMs from phase 5 of CMIP (CMIP5) to investigate future changes in lake-effect snowfall across the Great Lakes basin.

Here, output from two CMIP5 GCMs is dynamically downscaled for the late twentieth, mid-twenty-first, and late twenty-first centuries using a high-resolution RCM interactively coupled to a one-dimensional lake model; these are the same simulations examined by Notaro et al. (2015). RCM-based NBS perturbations are superimposed on the historical estimated NBS time series and used to force a Great Lakes channel model to develop lake level projections. The study addresses the following questions. 1) How will climate change alter the Great Lakes water supply? 2) Is a systematic increase or decrease in water levels expected? 3) Do projections agree across climate models with differing rates of projected increases in regional temperature and precipitation? 4) What are these projections' limitations? The data and methods, results, and summary and discussion are provided in sections 2, 3, and 4, respectively.

2. Data and methods

The following subsections describe the 1) applied datasets, 2) model configuration, 3) experimental design, 4) criteria for choosing which GCMs to downscale, and 5) methodology for producing lake level projections. A flow diagram of the applied model configuration is provided in Fig. S1 of the supplemental material.

a. Datasets

Monthly near-surface air temperature and precipitation output is obtained from historical (1980–99) and twenty-first-century (2040–59 and 2080–99) simulations of 33 CMIP5 GCMs (Taylor et al. 2012), according to the representative concentration pathway 8.5 (RCP8.5) scenario. This high forcing and emission scenario, with mostly unabated emissions, considers a continuous increase in radiative forcing, reaching 8.5 $W m^{-2}$ by 2100 (Moss et al. 2010; van Vuuren et al. 2011). The data are used to assess the range of climate projections across the Great Lakes region and evaluate the performance of individual CMIP5 models, leading to the selection of two GCMs to provide lateral boundary conditions (LBCs) to an RCM. The GCM- and RCM-outputted seasonal cycles of

near-surface air temperature and precipitation within the Great Lakes region are evaluated against gridded observational products [U. Delaware (Willmott and Matsuura 2000) and Maurer (Maurer et al. 2002)], along with a gauge-undercatchment corrected precipitation dataset (U. Del. undercatch; Adam and Lettenmaier 2003; Adam et al. 2006). The RCM-outputted seasonal cycles of lake surface temperatures (LSTs) and percent ice cover for the Great Lakes are evaluated against the National Oceanic and Atmospheric Administration (NOAA) Great Lakes Surface Environmental Analysis (GLSEA; Schwab et al. 1992) and Great Lakes Ice Atlas (Assel 2003, 2005; Wang et al. 2012), respectively. The RCM outputs daily ice thicknesses, as opposed to the ice atlas, which contains percent ice cover for each grid cell. For the purpose of comparison, based on daily model output, a lake grid cell is assigned 100% ice cover if the ice thickness is at least 2 cm or 0% otherwise. Clearly, there are concerns when comparing binary (0% or 100%) simulated ice fields to an observational product, which contains partial coverage between 0% and 100%. However, a nearly identical observed ice cover climatology is generated if the observations are treated as binary, in which, for each grid cell, days with less than 50% cover are assigned as 0% and days with at least 50% ice cover are assigned as 100%, thereby alleviating some data comparison concerns. The NOAA/GLERL Great Lakes monthly hydrologic dataset (Croley and Hunter 1994) contains monthly estimates of overlake precipitation, lake evaporation, and drainage basin runoff, with uncertainty estimates provided by DeMarchi et al. (2010); this dataset is applied to evaluate the RCM-simulated seasonal cycle of NBS and its components. The variables in order of lowest to highest uncertainty are runoff (from −9% to +23% for Great Lakes), overlake precipitation (from −20% to +30%), lake evaporation (from −35% to +35%), and total NBS (from −40% to +40%).

b. *Model description*

The Abdus Salam International Centre for Theoretical Physics (ICTP) Regional Climate Model, version 4 (RegCM4; Elguindi et al. 2011; Giorgi et al. 2012), is utilized to develop climate change projections for the Great Lakes basin. Its atmospheric dynamics are based upon the fifth-generation Pennsylvania State University–National Center for Atmospheric Research (NCAR) Mesoscale Model (Grell et al. 1994). The compressible, finite-difference model is restricted to hydrostatic balance. Its radiative transfer scheme follows that of the NCAR Community Climate Model, version 3 (Kiehl et al. 1996). The subgrid explicit moisture scheme (Pal et al. 2000) handles resolvable-scale precipitation and nonconvective clouds. Smaller-scale precipitation is parameterized using the Grell (1993) cumulus convection scheme with the Fritsch and Chappell (1980) cumulus closure scheme, given its superior performance in the study region (Notaro et al. 2013b). The applied model configuration utilizes the Biosphere–Atmosphere Transfer Scheme (BATS; Dickinson et al. 1986, 1993) for its LSM, with three soil layers and 20 land cover classes. BATS determines the impact of vegetation and interactive soil moisture on surface–atmosphere exchanges of water vapor, energy, and momentum. Its predictive equations for soil moisture consider precipitation, snowmelt, evapotranspiration, canopy foliage drip, surface runoff, infiltration below the root zone, and diffusive exchange of water across soil layers (Elguindi et al. 2011). Runoff is a function of precipitation rate and soil water content, relative to saturation (Steiner et al. 2005, 2009). Groundwater, base flow, or explicit rivers are not represented. Here, the RCM is configured with 25-km horizontal grid spacing over most of the United States and central-southern Canada (Fig. 1), with 28 vertical sigma layers.

RegCM4 is coupled to a one-dimensional energy-balance lake model (Hostetler and Bartlein 1990), with 1-m vertical resolution, to account for vertical heat transfer within a lake column by eddy diffusion and convective mixing/overturning. Horizontal heat transfer between neighboring lake points and vertical heat transfer between the lake bottom and lake water are not considered. These limitations cause deficiencies in simulated Great Lakes temperature and ice, given the lakes' dynamic circulations (Bennington et al. 2014). BATS computes lake–atmosphere fluxes of sensible and latent heat using the bulk aerodynamic formulas (Dickinson et al. 1993). The lake ice submodel (Patterson and Hamblin 1988; Hostetler 1991) represents heat and moisture exchanges between the atmosphere and both open water and ice surfaces and computes the surface energy of lake ice and overlying snow. Time-invariant two-dimensional lake depths are assigned according to bathymetry from a 30-arc-s Earth topography dataset (ETOPO; Amante and Eakins 2009). Several corrections (Notaro et al. 2013b; Bennington et al. 2014) are applied to the lake model, related to calculation of shortwave extinction coefficients, lake heating by shortwave radiation, generation of local mixing around unstable layers, intensity of eddy diffusion within deep lake points, and energy conservation within ice melting and growth computations.

The performance of RegCM4, including its predecessors, and its lake model has been extensively evaluated for the Great Lakes basin (Hostetler et al. 1993; Bates et al. 1995; Martynov et al. 2010; Holman et al. 2012; Notaro et al. 2013a,b, 2015; Bennington et al. 2014).

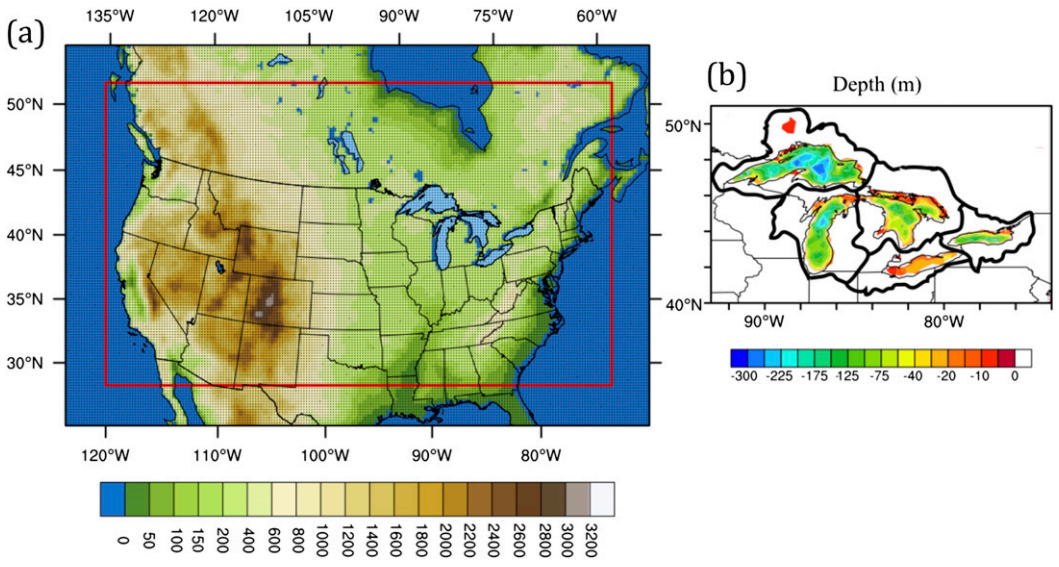

FIG. 1. (a) RCM domain, with shading for elevation (m) and small dots for the 25-km grid points. The inner domain, within the buffer zone, is shown with the red box. (b) Lake depth (shown as negative elevation; m) and outline of each drainage basin.

When provided LBCs from reanalysis, the model generally reproduces the seasonal cycle of LSTs compared to buoy and remote sensing data, although with a summertime warm bias and anomalously early stratification (Bennington et al. 2014; Notaro et al. 2015). RegCM4 produces a fair representation of the spatial distribution and seasonal evolution of lake ice cover, but the absence of horizontal mixing and ice movement causes an excessive and overly persistent ice cover (Notaro et al. 2013b, 2015). Based on a reanalysis-forced simulation, Notaro et al. (2013b) found biases in October–May mean ice cover, which ranged from +11% for Lake Huron to +20% for Lake Superior, coinciding with a mean ice duration that exceeded observations by 13 and 32 days, respectively. The model simulates a reasonable spatial pattern of annual snowfall, including the lake-effect snow regions (Notaro et al. 2013b). It accurately simulates the interannual fluctuations and long-term historical trends in basinwide air temperatures, lake ice cover, and snowfall (Notaro et al. 2013b). The reanalysis-driven RegCM4 simulation of Notaro et al. (2013b) exhibited a temporal correlation of 0.95 compared to the Great Lakes Ice Atlas in terms of the time series of mean Great Lakes ice cover for December–May during 1976/77–2001/02, with close agreement between the observed ($-0.75\%\ \mathrm{yr}^{-1}$) and simulated ($-0.70\%\ \mathrm{yr}^{-1}$) ice cover trends.

c. *Experimental design*

The RegCM4 simulations apply 25-km grid spacing for a domain of 217×141 grid cells, covering most of the continental United States and southern Canada (Fig. 1). The Great Lakes are represented by 431 grid cells. LBCs are provided to a 15 gridcell buffer zone, surrounding the inner domain, according to a linear relaxation scheme. RegCM4 is applied to dynamically downscale both historical and future simulations, according to RCP8.5, from two CMIP5 GCMs: the Model for Interdisciplinary Research on Climate, version 5 (MIROC5), and the Centre National de Recherches Météorologiques Coupled Global Climate Model, version 5 (CNRM-CM5). The RCM-MIROC5 and RCM-CNRM simulations are produced for the late twentieth (1970–99), mid-twenty-first (2030–59), and late twenty-first (2070–99) centuries. For each period, lake temperatures are initialized uniformly at 4°C, followed by a 10-yr spinup. The last 20 years are analyzed per period. The Great Lakes are crudely represented by these GCMs. In MIROC5 (Watanabe et al. 2010), only 12 grid cells in the actual Great Lakes basin are assigned at least 50% water. The Matsiro LSM (Takata et al. 2003) within MIROC5 includes a simple lake submodel with one surface layer and four subsurface layers. In CNRM-CM5, the Great Lakes are represented by 10 grid cells, with at least 50% water (Voldoire et al. 2013). Within CNRM-CM5's Surface Externalisée (SURFEX) interface, LSTs are updated through extrapolation from the nearest ocean grid cell. Despite the limitations of a one-dimensional lake model, the high-resolution coupled RegCM4–lake model is a clear advance over the Great Lakes' depiction in either GCM in terms of horizontal and vertical resolution and represented processes.

d. Criteria for selecting GCMs to downscale

Given the vast number of GCMs that may be utilized to provide LBCs for dynamical downscaling and the sensitivity of lake level projections to the choice of GCM, an objective GCM selection for downscaling is applied here (supplemental Table 1 of Notaro et al. 2015). The initial pool consists of 33 CMIP5 GCMs (Taylor et al. 2012). GCMs are considered only for the available 6-hourly fields, needed as LBCs for RegCM4—namely, zonal and meridional wind, air temperature, humidity, and surface pressure. The GCM must have sufficiently high spatial resolution to avoid a large ratio (10:1 or greater) between the resolution of the parent GCM and RCM (Denis et al. 2002; Antic et al. 2004). The five coarsest models, with 2.81° × 2.81° resolution, are eliminated, as they exceed the 10:1 ratio. MIROC5 and CNRM-CM5 have 1.4° × 1.4° resolution, leading to a ratio of 5.3:1 between the parent GCM and 25-km RCM.

Although past studies have reached contradictory conclusions regarding the importance of an accurately simulated twentieth-century climatology to credible future climate projections (Reifen and Toumi 2009; Dominguez et al. 2010), we have chosen to evaluate the historical performance of the CMIP5 models within the Great Lakes region (40°–50°N, 70°–95°W) in order to eliminate models with excessive regional biases. For example, if a GCM with a large warm bias is downscaled, minimal historical lake ice cover may be simulated, which will limit the potential magnitude of future lake ice decline and its consequence on regional climate through lake–atmosphere feedbacks. The seasonal cycles of simulated historical overland annual precipitation and air temperature within the region are compared to observational products, namely U. Delaware, Maurer, and U. Del. undercatch. Root-mean-square differences (RMSDs) are calculated for each CMIP5 GCM for the mean seasonal cycles of both air temperature and precipitation (based on 12 monthly mean values per variable), compared to observations. The mean RMSDs for temperature and precipitation, averaged among the models, are 1.8°C and 0.52 mm day^{-1}, respectively. As a result of poor representation of regional-mean climatology, 11 GCMs are eliminated from the reduced pool of 28 models. Specifically, the models' RMSD for the temperature seasonal cycle and RMSD for the precipitation seasonal cycle are both normalized and averaged, leading to a metric that represents the models' overall regional climate performance; 11 models with higher-than-average (from the full set of 33 models) mean normalized RMSD are eliminated, thereby reducing the pool to 17 models. We decided to select two GCMs that simulate close to the average increase in annual precipitation by the late twenty-first century among the CMIP5 models but represent a range of potential warming (Notaro et al. 2015). Ongoing downscaling efforts are expanding this pool. Of the remaining 17 models, 11 are eliminated given that their projected change in basinwide annual precipitation is beyond ±0.5 standard deviation (σ) of the models' mean projection. Of the six remaining models, MIROC5 is chosen as a high-end warming model, specifically the only one with a peak projected warming in spring, and CNRM-CM5 is chosen as a low-end warming model, with typical (within CMIP5) peak warming in winter.

Projected changes in air temperature and precipitation, based on comparing the historical twentieth-century simulations (1980–99) and transient twenty-first-century simulations (2040–59 and 2080–99) according to the RCP8.5 scenario, are computed for each CMIP5 model across the Great Lakes region (Fig. 2). The vast majority of CMIP5 models produce a regional increase in annual air temperature and precipitation. Annual-mean precipitation is projected by the CMIP5 GCMs to regionally increase at a rate of +2.2% °C^{-1} of warming by the late twenty-first century (+2.6% °C^{-1} in CNRM-CM5 and +1.6% °C^{-1} in MIROC5), averaged across the models, which is in line with the projections from Held and Soden (2006) and Stephens and Ellis (2008). The largest model-mean projected warming occurs in December–February (DJF) at +3.8°C (±1.3°C for 1σ as a measure of across-model spread in projected seasonal temperature change) by the mid-twenty-first century and 7.0°C (±1.7°C) by the late twenty-first century. The largest model-mean increase in precipitation occurs in March–May (MAM) at +0.32 mm day^{-1} (±0.16 mm day^{-1}) by the mid-twenty-first century and +0.61 mm day^{-1} (±0.28 mm day^{-1}) by the late twenty-first century. CNRM-CM5 and MIROC5 are selected for having internally consistent projections for both periods and a unique distribution of future responses in temperature and precipitation. By the late twenty-first century, CNRM-CM5 and MIROC5 simulate an annual warming of +5.3° and 7.1°C and an increase in annual precipitation of +0.35 and +0.32 mm day^{-1}, respectively. Their late twenty-first-century projections are most dissimilar in MAM, with projected warming of 4.1°C in CNRM-CM5 and +8.8°C in MIROC5 and projected increase in precipitation of +0.68 mm day^{-1} in CNRM-CM5 and +0.53 mm day^{-1} in MIROC5.

Hereafter, GCM-CNRM and GCM-MIROC5 refer to the CMIP5 GCMs CNRM-CM5 and MIROC5, and RCM-CNRM and RCM-MIROC5 refer to their downscaled simulations using RegCM4.

e. Developing lake level projections

The Great Lakes water levels are determined by the NBS for individual lakes and the connecting channel

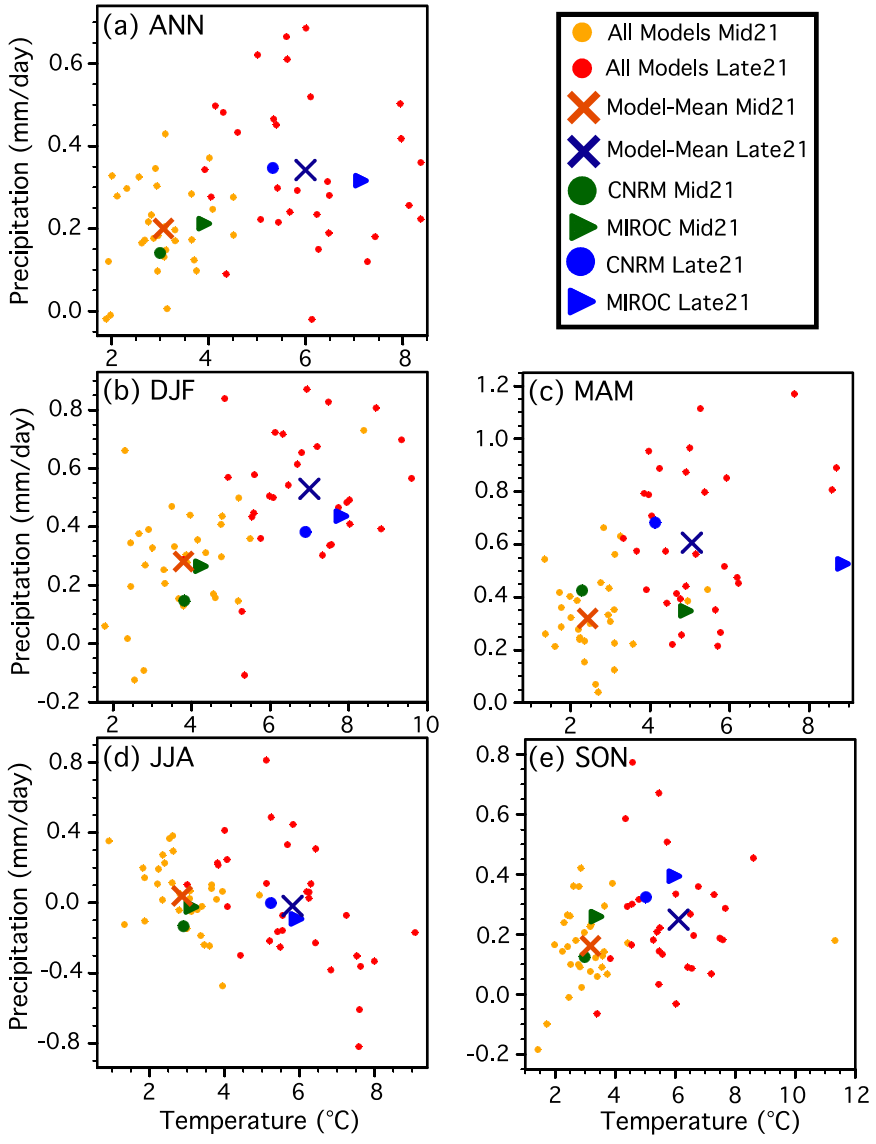

FIG. 2. Projected changes in 2-m air temperature (°C) and precipitation (mm day^{-1}), both (a) annually and (b)–(e) by season, across the Great Lakes region (40°–50°N, 95°–70°W; land only), computed as the difference between either 2040–59 or 2080–99 and 1980–99. Each dot represents one of 33 CMIP5 GCMs for mid-twenty-first- (orange) or late twenty-first- (red) century projections. Model-mean projections are shown for the mid- and late twenty-first century with brown and blue crosses, respectively. Projections from GCM-CNRM (large dot) and GCM-MIROC5 (sideways triangle) are identified with green and blue symbols for the mid-twenty-first and late twenty-first century, respectively.

flow between lakes. The NBS for each lake is defined as the sum of the overlake precipitation and drainage basin runoff minus lake evaporation. Each lake's drainage basin is larger than the lake's surface area; therefore, if precipitation rates are equal over land and lake, then the water accumulated over land will add a greater mass of water to the lake. The impact of runoff on lake depth is computed by multiplying the runoff per area by the ratio of the corresponding basin area to lake area.

A treaty between the United States and Canada regulates the channel flow between Lakes Superior and Huron and out of Lake Ontario. The Lake Superior regulation and routing module determines the human-controlled flow out of Lake Superior and includes the Ogoki and Long Lac diversions into the lake, as well as total Superior outflow and the permitted minima and maxima in side channel outflow. This model is combined with a coordinated hydrologic response model for the middle Great Lakes, the

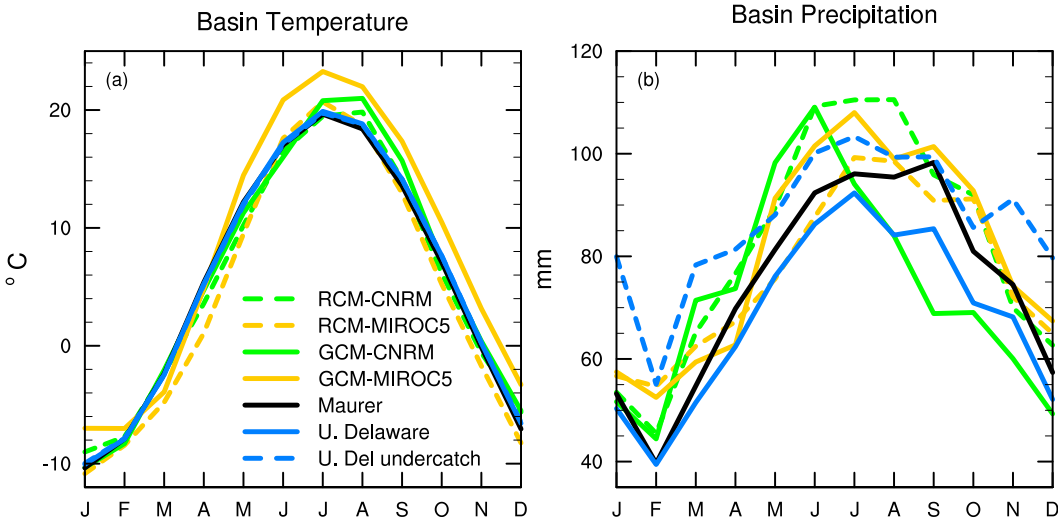

FIG. 3. Mean seasonal cycles of (a) near-surface air temperature (°C) and (b) precipitation (mm) over land within the Great Lakes basin (40°–50°N, 70°–95°W) for 1980–99. Data sources include the RCM simulations (RCM-CNRM and RCM-MIROC5), parent GCM simulations (GCM-CNRM and GCM-MIROC5), and observations [Maurer (Maurer et al. 2002), U. Delaware (Willmott and Matsuura 2000), and U. Del undercatch (Adam and Lettenmaier 2003, Adam et al. 2006)]. The models are evaluated only over land, given the lack of overlake observations considered by these gridded observational products.

middle lakes (MIDLAKES) model. The resulting hydrologic routing model, known as the Coordinated Great Lakes Regulation and Routing Model (CGLRRM; Quinn 1978; Clites and Lee 1998), which was developed by NOAA/GLERL, U.S. Army Corps of Engineers, and Environment Canada and applied by GLERL in experimental forecasting, is used here to produce monthly mean water level projections for Lakes Superior, Michigan–Huron, St. Clair, and Erie when provided initial water level conditions and RegCM4-outputted NBS components for each lake. CGLRRM considers diversions out of the basin, including the Chicago diversion and Welland Canal. The faulty evapotranspiration calculation by the GLERL suites (Lofgren et al. 2011) is not a concern here, as RegCM4-outputted evapotranspiration is provided to CGLRRM, with the application of CGLRRM primarily limited to determining water routing between the lakes and resulting lake levels. Lake Ontario's regulation model is currently not operational, so water level projections are not made for that lake. To reduce NBS biases inputted into the channel model, the mean and standard deviation in RCM-based projected changes in NBS are utilized to perturb historical-mean NBS estimates from the Great Lakes monthly hydrologic dataset for 1948–2006. Within CGLRRM, groundwater acts as a temporary storage reservoir, which eventually drains into the lakes, and does not affect the overall water budget but instead just the timing of water's release into the lake (Lofgren et al. 2002).

Projected lake levels are obtained by perturbing the historical-mean NBS with the mean and standard deviation in RCM-based projected changes in NBS and then inputting these projected NBS values into CGLRRM. Historical NBS estimates for 1948–2006 are obtained from the Great Lakes monthly hydrologic dataset. To simulate extreme water levels, the autocorrelation and cross correlations are calculated for the GLERL estimates of the components of historical NBS. The monthly mean components of NBS are then adjusted by the RCM projected changes. While preserving both the autocorrelation and cross correlation from the observed period, 1000 18-yr samples of NBS are completed by random sampling of the projected monthly components. The randomized NBSs are inputted into the water level model and used to project likely extremes in water levels.

3. Results

After quantifying added value resulting from dynamical downscaling and evaluating simulated LSTs, lake ice, and NBS against observations and best available estimates in sections 3a–d, projected changes in regional climate, NBS, and lake levels are described in sections 3e–g.

a. Added value from dynamical downscaling

Dynamical downscaling adds value relative to the two CMIP5 models in terms of their mean seasonal cycles of near-surface air temperature and precipitation across the Great Lakes region, particularly for GCM-MIROC5 (Fig. 3). GCM-CNRM outperforms GCM-MIROC5 regarding

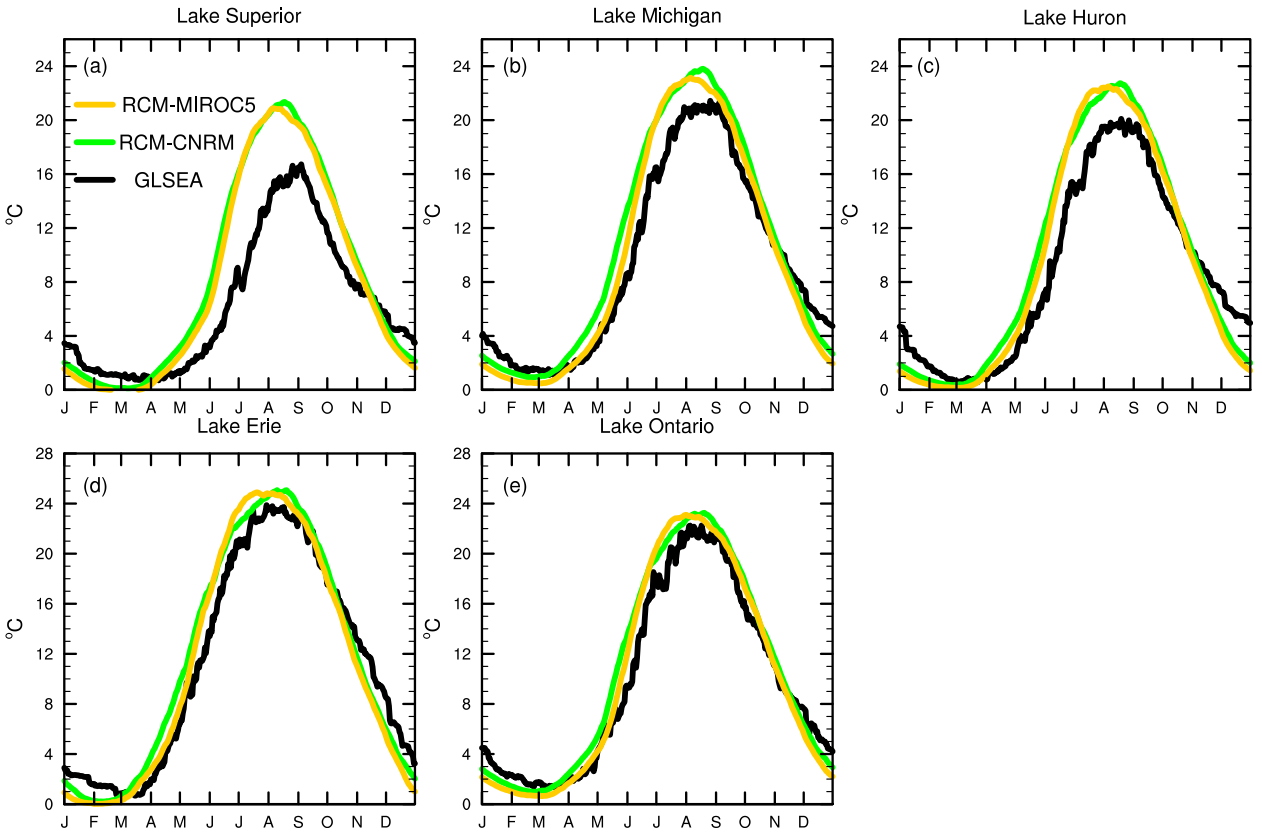

FIG. 4. Mean seasonal cycle of daily LSTs (°C) from GLSEA (black; 1995–2000), RCM-MIROC5 (yellow; 1980–99), and RCM-CNRM (green; 1980–99) for Lakes (a) Superior, (b) Michigan, (c) Huron, (d) Erie, and (e) Ontario. In the model, when ice is present, outputted LSTs represent the water temperatures under the ice, which remain above freezing.

temperature's seasonal cycle, while GCM-MIROC5 outperforms GCM-CNRM regarding precipitation. Downscaling of GCM-MIROC5 with RegCM4 results in a 34% reduction in the RMSD in the monthly temperature seasonal cycle, compared to the monthly climatology averaged between the Maurer and U. Delaware datasets, with a notable reduction in the June–August (JJA) warm bias. Since GCM-CNRM already performs exceptionally well in terms of temperature's seasonal cycle, downscaling in RCM-CNRM reduces the RMSD by only 3%. Regarding precipitation's seasonal cycle, downscaling results in a 42% reduction in the RMSD from GCM-CNRM and minimal change in RMSD from GCM-MIROC5 compared to the monthly climatology averaged between the uncorrected Maurer dataset and U. Del. undercatch dataset. RegCM4 reduces the dry bias during July–February in GCM-CNRM. The number of months that lie within the range of observational uncertainty for precipitation (based on the three aforementioned datasets) is increased from 5 to 7 by downscaling GCM-CNRM and from 7 to 11 by downscaling GCM-MIROC5. The most pronounced biases in RCM-CNRM are a cold bias of −1.8°C during April–May and wet bias of +12 mm month^{-1} during June–August. The largest biases in RCM-MIROC5 are a −3.1°C cold bias during March–May and a +9 mm month^{-1} wet bias during April–June.

b. *Evaluation of simulated LSTs*

The simulated seasonal cycle of LSTs in RCM-CNRM and RCM-MIROC5 is evaluated against GLSEA (Fig. 4). The RCM captures the key characteristics of the LST seasonal cycle. However, the absence of lake circulations and explicit three-dimensional lake mixing causes an anomalously early onset of stratification, an exaggerated spring–early summer rate of warming, and a summer warm bias, consistent with prior studies (Martynov et al. 2010, 2012; Bennington et al. 2014; Notaro et al. 2013a,b, 2015). The model generally produces a large warm bias in April–September and modest cold bias in November–February. LSTs are poorly simulated for deep lakes, particularly Lake Superior with a peak warm bias of 7°–8°C in July. In terms of the RMSD between the long-term-mean simulated and observed seasonal cycle in LSTs (12 monthly values per lake), Lake Ontario is well captured (RSMD of 1.75°C in RCM-CNRM and 1.66°C in RCM-MIROC5) and Lake Superior is poorly

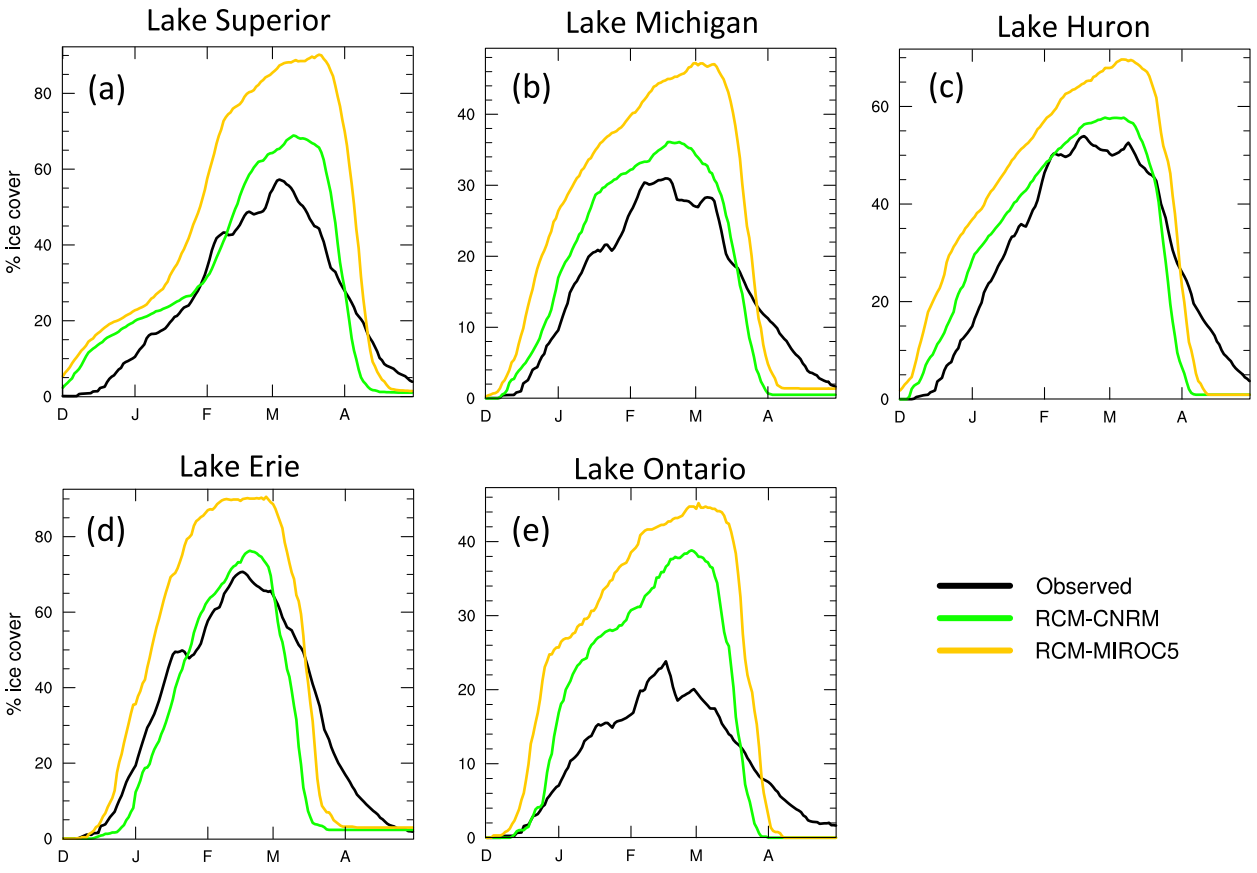

FIG. 5. Mean seasonal cycle of daily percent lake ice cover for Lakes (a) Superior, (b) Michigan, (c) Huron, (d) Erie, and (e) Ontario from the Great Lakes Ice Atlas (black), RCM-MIROC5 (yellow), and RCM-CNRM (green) for 1980–99.

simulated (RMSD of 3.81°C in RCM-CNRM and 3.59°C in RCM-MIROC5). Simulated LSTs generally peak too early compared to GLSEA, with 10–15 days bias for Lake Superior. The cold bias during December–April is about 0.5°–1.0°C greater in RCM-MIROC5 than RCM-CNRM, leading to excessive ice cover in RCM-MIROC5.

c. *Evaluation of simulated lake ice*

The absence of horizontal mixing and ice motion in the lake model leads to early ice onset, excessive mid-winter ice development (especially for Lakes Superior and Ontario), and abrupt spring melt (Fig. 5) (Notaro et al. 2013b, 2015). RCM-CNRM outperforms RCM-MIROC5 for every lake, except Erie, as evident by a lower RMSD of the long-term-mean simulated seasonal cycle (151 daily values per lake during December–April) of percent ice cover compared to the Great Lakes Ice Atlas. This RMSD is smallest for Lake Michigan (5.8% for RCM-CNRM and 13.0% for RCM-MIROC5) and greatest for Lake Superior (10.3% for RCM-CNRM and 25.4% for RCM-MIROC5). Simulated ice forms too early for most lakes, reaching 10% cover on Lake Superior on average 20 days too early in RCM-CNRM and 24 days too early in RCM-MIROC5 compared to observations. Furthermore, the simulated lake ice season ends too early, with pronounced April biases on Lake Huron of −11.7% for RCM-CNRM and −9.0% for RCM-MIROC5.

It is noted that the minimum daily ice thickness requirement of 2 cm for assigning 100% ice cover to a grid cell is somewhat arbitrary. However, changing this threshold results in only minor changes to the computed seasonal cycle of lake ice cover. For example, the December–April mean ice cover on Lake Superior ranges from 30.8% if a 1-cm threshold is applied to 29.5% if a 5-cm threshold is applied in RCM-CNRM output, and from 46.1% if a 1-cm threshold is applied to 44.4% if a 5-cm threshold is applied in RCM-MIROC5 output.

Biases in LST and lake ice cover are compared between RegCM4, interactively coupled to the Hostetler and Bartlein (1990) lake model, and the Weather Research and Forecasting (WRF) Model, forced by lake

conditions derived through an offline coupling with the two-layer freshwater lake model as applied by Gula and Peltier (2012). Compared to GLSEA, annual LSTs are biased too high for all of the Great Lakes in RegCM4 and too low for Lakes Ontario and Erie in WRF. LST biases are larger in RegCM4 than WRF for Lakes Superior, Huron, and Michigan, equal in magnitude between the models for Lake Ontario, and larger in WRF for Lake Erie. LSTs are generally too low during winter and too high during spring in both models. Mallard et al. (2014) later developed a version of WRF that was interactively coupled to the freshwater lake (FLake) model and forced by reanalysis, which slightly reduced the simulated LST biases but instead exhibited warm biases outside of the cold season and annual-mean biases on the order of 2°–3°C. Compared to the Great Lakes Ice Atlas, excessive ice cover is simulated by RegCM4 on Lakes Superior and Ontario and by WRF on all of the lakes. In summary, both RCMs display significant LST and ice cover biases resulting from limitations of applying one-dimensional lake models and climate biases in the parent GCM.

d. Evaluation of simulated NBS

The mean seasonal cycles of overlake precipitation, runoff, lake evaporation, and total NBS in the Great Lakes basin from RCM-CNRM and RCM-MIROC5 are evaluated against the Great Lakes monthly hydrologic dataset (Fig. 6), while recognizing the sizeable uncertainty in this dataset (DeMarchi et al. (2010)). The seasonal cycle of overlake precipitation is well captured, including the late summer–early autumn peak, as simulated monthly precipitation falls within the range of observational uncertainty for every month in both model configurations. Mean annual overlake precipitation in RCM-CNRM (886 mm) and RCM-MIROC (860 mm) closely matches GLERL's estimates (862 mm).

Overland precipitation that runs off into the lakes is underestimated by RegCM4 during winter, potentially due to the absence of groundwater, base flow, and explicit rivers in the model. While both model configurations capture the snowmelt-related runoff peak in March–May, their annual runoff is too low by 86 mm in RCM-CNRM and 106 mm in RCM-MIROC5, particularly in winter. Only five and four months lie within the range of observational uncertainty in runoff's seasonal cycle from RCM-CNRM and RCM-MIROC5, respectively.

Simulated lake evaporation is the most problematic NBS component, with an unreasonable seasonal cycle that includes a simulated peak that occurs three months earlier than in GLERL's estimates. For both RCM-CNRM and RCM-MIROC5, only three months of simulated lake evaporation fall within the range of observational uncertainty. However, the annual-mean lake evaporation is reasonable and only slightly greater than GLERL estimates by 63 mm in RCM-CNRM and 14 mm in RCM-MIROC5. Deficiencies in simulated LSTs, including early stratification and warm-up and large summertime positive LST biases, partly explain the excessive simulated summertime lake evaporation but do not fully explain the shift in its seasonal cycle. For example, LSTs on Lake Erie peak in August in both RegCM4 and GLSEA, yet lake evaporation peaks in August in RegCM4 and October in the GLERL estimates. Either overlake vapor pressure or wind speed is likely inadequately simulated, indicating an atmospheric model deficiency that requires further investigation. Observations from Stannard Rock lighthouse have verified the December–February peak in lake evaporation resulting from strong winds and low atmospheric vapor pressure (Blanken et al. 2011).

RegCM4 captures the April peak in NBS, but as a result of insufficient annual runoff, the simulated annual NBS is too low by 126 mm (−13%) in RCM-CNRM and 123 mm (−13%) in RCM-MIROC5. Seven months of simulated monthly NBS fall within the range of observational uncertainty for both model configurations. Simulated NBS is too low during July–September because of excessive lake evaporation.

e. Regional climate projections

The discussion here focuses on projected changes in critical variables within the Great Lakes region (Fig. 7) that affect hydrology, NBS, and lake levels. Similar to their parent GCMs, RCM-MIROC5 simulates a greater projected warming than RCM-CNRM, particularly in spring. Annual overland air temperatures increase by +2.2°C in RCM-CNRM and +3.0°C in RCM-MIROC5 by the mid-twenty-first century and by +4.2°C in RCM-CNRM and +5.9°C in RCM-MIROC5 by the late twenty-first century. The land surface warms more annually than lake surfaces by approximately 33%, in general, as a result of the land's lower heat capacity. Unlike that of land surface temperature, the projected LST change has a distinct seasonal cycle, with peak warming in May–July related to earlier lake stratification. For May–June, the lake surfaces warm by +2.4°C in RCM-CNRM and +3.2°C in RCM-MIROC5 by the mid-twenty-first century and by +4.9°C in RCM-CNRM and +7.1°C in RCM-MIROC5 by the late twenty-first century. In response to warming, the two model configurations produce similar reductions in lake ice cover, with maximum declines in February–March. RCM-MIROC5 simulates reductions in percent ice cover of −9.9% and −20.1% by the mid- and late twenty-first century,

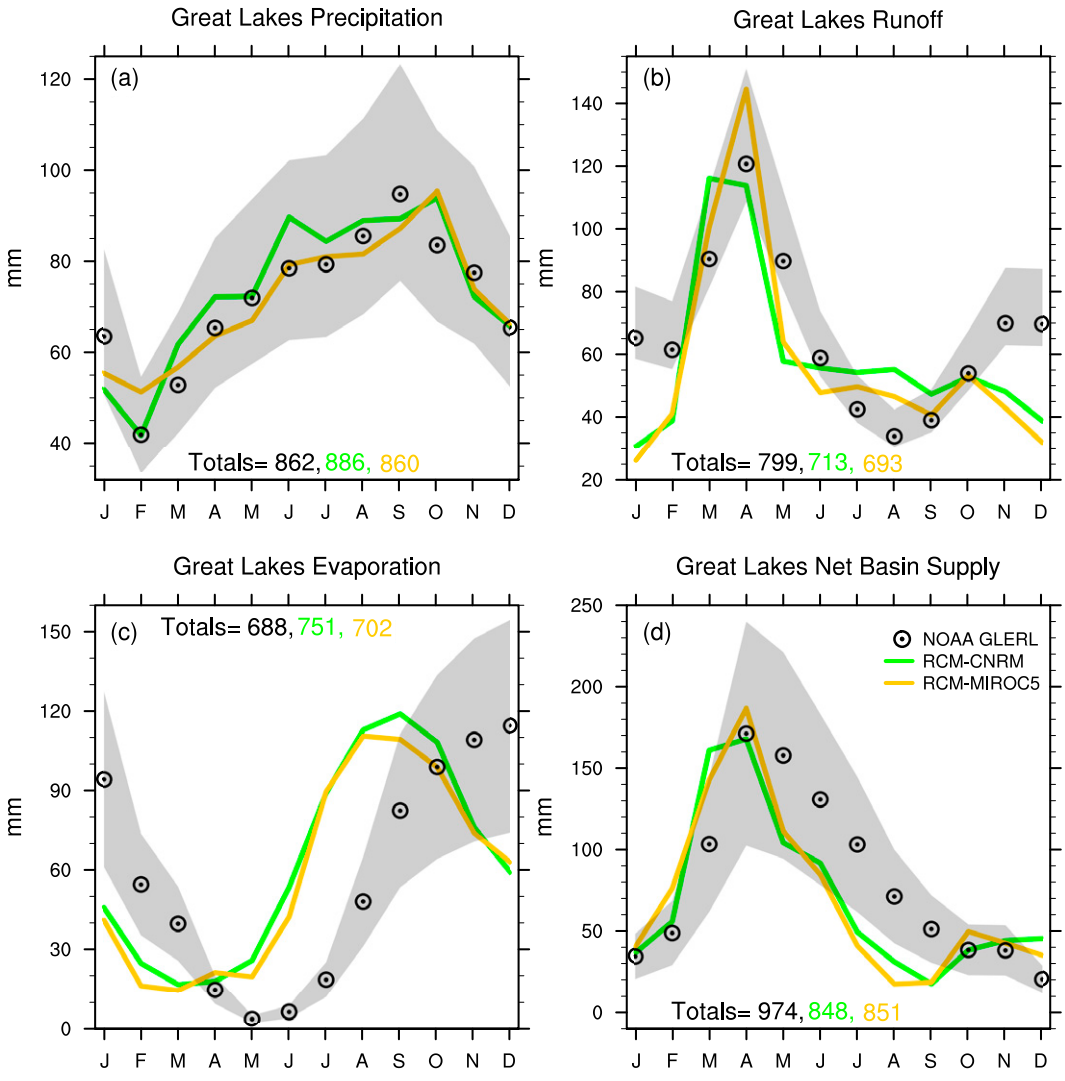

FIG. 6. Mean seasonal cycles of (a) overlake precipitation, (b) basin runoff, (c) lake evaporation, and (d) NBS in millimeters of lake depth from NOAA/GLERL (black dots with shading for uncertainty estimates), RCM-CNRM (green), and RCM-MIROC5 (yellow) for 1980–99. Annual totals of NBS and each component (millimeters of lake depth) are denoted for NOAA estimates and RCM results in corresponding text color. Uncertainties in the GLERL data for Lakes Erie and Michigan are obtained from DeMarchi et al. (2010).

respectively. By the late twenty-first century, lake ice becomes mainly confined to the northern shores, with open water across most of the lakes even in midwinter, as also noted by Notaro et al. (2015).

Both model configurations indicate projected increases in annual precipitation, with notably larger increases in RCM-CNRM, particularly in late winter to spring. Annual precipitation in the Great Lakes region increases at rates of +3.6% $°C^{-1}$ of surface warming in RCM-CNRM and +1.5% $°C^{-1}$ in RCM-MIROC5 by the mid-twenty-first century and at rates of +3.7% $°C^{-1}$ in RCM-CNRM and +1.7% $°C^{-1}$ in RCM-MIROC5 by the late twenty-first century, which are similar rates to those produced by the CMIP5 GCMs. If limited to days with precipitation, then precipitation intensity in the Great Lakes region increases by +7.1% and +5.7% $°C^{-1}$ by the mid-twenty-first century and +7.3% and +4.8% $°C^{-1}$ by the late twenty-first century for RCM-CNRM and RCM-MIROC5, respectively. Furthermore, if only extreme precipitation days are considered, representing the top 1% of precipitation days during 1980–99, then the rates are +7.6% and +7.3% $°C^{-1}$ by the mid-twenty-first century and +8.4% and +6.6% $°C^{-1}$ by the late twenty-first century for RCM-CNRM and RCM-MIROC5, respectively. Pall et al. (2007) previously suggested that the estimated rate of +7% $°C^{-1}$, based on the

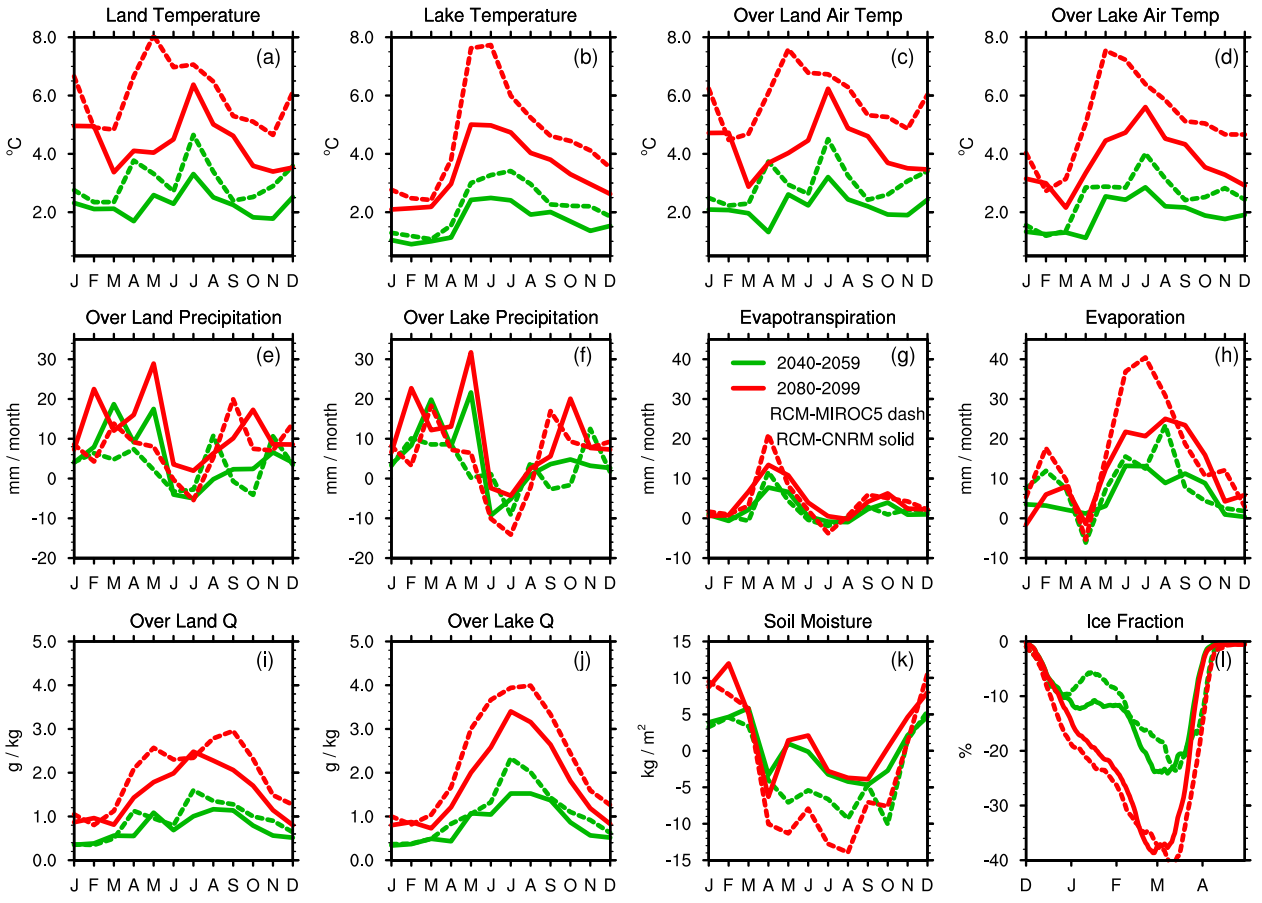

FIG. 7. RCM-based projected changes in key variables within the Great Lakes basin, according to RCM-MIROC5 (dashed) and RCM-CNRM (solid), by the mid-twenty-first century (2040–59; green) and late twenty-first century (2080–99; red) compared to the late twentieth century (1980–99). Variables include monthly (a) land surface temperature (°C), (b) LST (°C), (c) overland air temperature (°C), (d) overlake air temperature (°C), (e) overland precipitation (mm month^{-1}), (f) overlake precipitation (mm month^{-1}), (g) overland evapotranspiration (mm month^{-1}), (h) lake evaporation (mm month^{-1}), (i) overland specific humidity (g kg^{-1}), (j) overlake specific humidity (g kg^{-1}), (k) deep soil moisture in the root zone (kg m^{-2}), and (l) daily percent Great Lakes ice cover.

Clausius–Clapeyron relationship, was likely a reliable predictor of changes in extreme precipitation, perhaps even more reliable than for mean precipitation changes. However, given that changes in atmospheric circulation can also affect future changes in regional precipitation extremes, the estimated rate from Pall et al. (2007) could be considered as overly simplified. Yet dynamical downscaling experiments for the Great Lakes region using WRF, produced by d'Orgeville et al. (2014) and using RegCM4, as presented here, yielded rates of increase in both mean rainfall on rainy days and in extreme rainfall intensities that closely matched this +7% °C^{-1} rate.

Annual overland precipitation increases by +63 mm in RCM-CNRM and +39 mm in RCM-MIROC5 by the mid-twenty-first century and by +143 mm in RCM-CNRM and by +92 mm in RCM-MIROC5 by the late twenty-first century. Overland precipitation is generally projected to increase during most months, particularly February–May, but decrease in June–July. During June–July, RegCM4 produces slight reductions in overland precipitation and more substantial drying over the lakes. By the late twenty-first century, RCM-MIROC5 shows minor reductions in overland precipitation of −3 mm month^{-1} during June–July, compared to moderate overlake reductions of −12 mm month^{-1}. This spatially heterogeneous precipitation response occurs since the lakes induce a greater warm-season stabilizing effect on the atmosphere in the late twenty-first-century than historically. The lakes' signature of cooling, higher pressure, sinking motion, and reduced boundary layer height, based on comparing overlake and overland variables within the basin, is amplified by the late twenty-first century.

Within RegCM4's late-twentieth-century simulations, snow depth in the Great Lakes region peaks during February–March, with peak snowmelt in March–April.

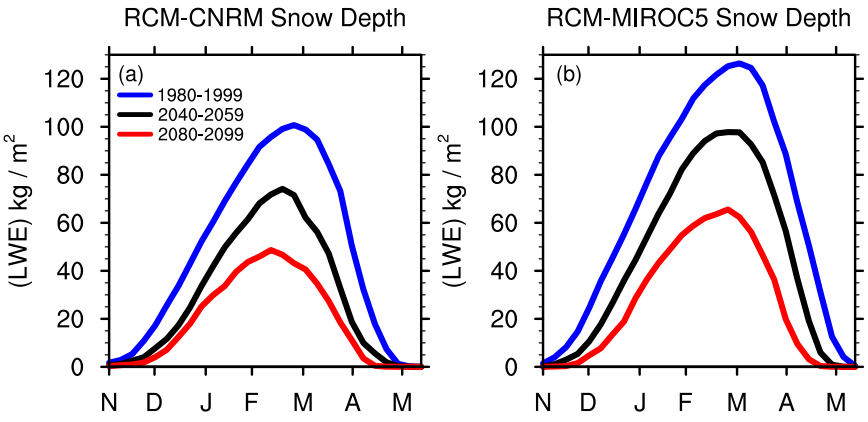

FIG. 8. Seasonal cycle (November–May) of weekly liquid water equivalent (LWE) of snow depth ($kg\,m^{-2}$) within the Great Lakes basin for the late twentieth (blue; 1980–99), mid-twenty-first (black; 2040–59), and late twenty-first (red; 2080–99) centuries from (a) RCM-CNRM and (b) RCM-MIROC5.

Regarding the liquid equivalent of snowpack for December–April, RCM-CNRM and RCM-MIROC5 simulate reductions of −30% and −37%, respectively, by the mid-twenty-first century, and both models agree on −59% reductions by the late twenty-first century (Fig. 8).

Projected increases in annual overland evapotranspiration are nearly identical between the two model configurations, at about +24 and +52 mm by the mid- and late twenty-first century, respectively. The seasonal cycle of projected changes in overland evapotranspiration exhibits a dual peak, with the largest increases in April–May, potential reductions in July–August, and modest increases in September–October, reflecting both moisture-limited evapotranspiration conditions and reduced or nearly unchanged precipitation. RCM-MIROC5 simulates annual reductions in both upper and lower soil moisture fraction by the mid- and late twenty-first century, with pronounced reductions in spring (reduced snowmelt) and summer (reduced precipitation) and increases in winter (greater precipitation). In contrast, RCM-CNRM produces annual reductions in upper soil moisture, especially in spring resulting from reduced snowmelt, and annual increases in lower soil moisture, especially in winter resulting from greater precipitation. Rising LSTs in both configurations lead to increases in annual lake evaporation, particularly in June–September, with greater annual increases by the late twenty-first century in RCM-MIROC5 (+196 mm) than RCM-CNRM (+140 mm) given its larger lake warming. Higher air temperatures support increased atmospheric saturation vapor pressure and total specific humidity, particularly in July–September and most distinctly in RCM-MIROC5. Annual increases in near-surface specific humidity by the late twenty-first century range from $+1.77\,g\,kg^{-1}$ in RCM-CNRM to $+2.31\,g\,kg^{-1}$ in RCM-MIROC5.

f. *Projected NBS changes*

Projected changes in NBS and its individual components are examined for the Great Lakes basin (Figs. 9–11). Both model configurations generally produce increases in annual overlake precipitation, lake evaporation, and basinwide runoff, but the relative magnitudes of these changes determine the combined impact on NBS and lake levels. For RCM-MIROC5, the basinwide, annually averaged projected changes in overlake precipitation, lake evaporation, and runoff are +36, +96, and +24 mm of lake depth, respectively, by the mid-twenty-first century and +60, +195, and +64 mm of lake depth, respectively, by the late twenty-first century. For RCM-CNRM, the projected changes in these variables are +62, +70, and +66 mm, respectively, by the mid-twenty-first century and +122, +141, and +154 mm, respectively, by the late twenty-first century.

In response to a dramatic rise in lake temperatures by RCM-MIROC5, the increase in annual lake evaporation exceeds the projected changes in the other NBS components (Fig. 9). RCM-MIROC5 produces more modest precipitation changes than RCM-CNRM, with significant changes primarily confined to Lake Superior. Runoff is projected to increase in December–February because of greater precipitation and decrease in April–May because of diminished snowpack and associated melt. The largest increases in lake evaporation occur in June–September. The combined impact of these changes in RCM-MIROC5 is a change in NBS ranging from −94 mm on Lake Ontario to +19 mm on Lake Superior by the mid-twenty-first century and from −127 mm on Lake Erie to +3 mm on Lake Ontario

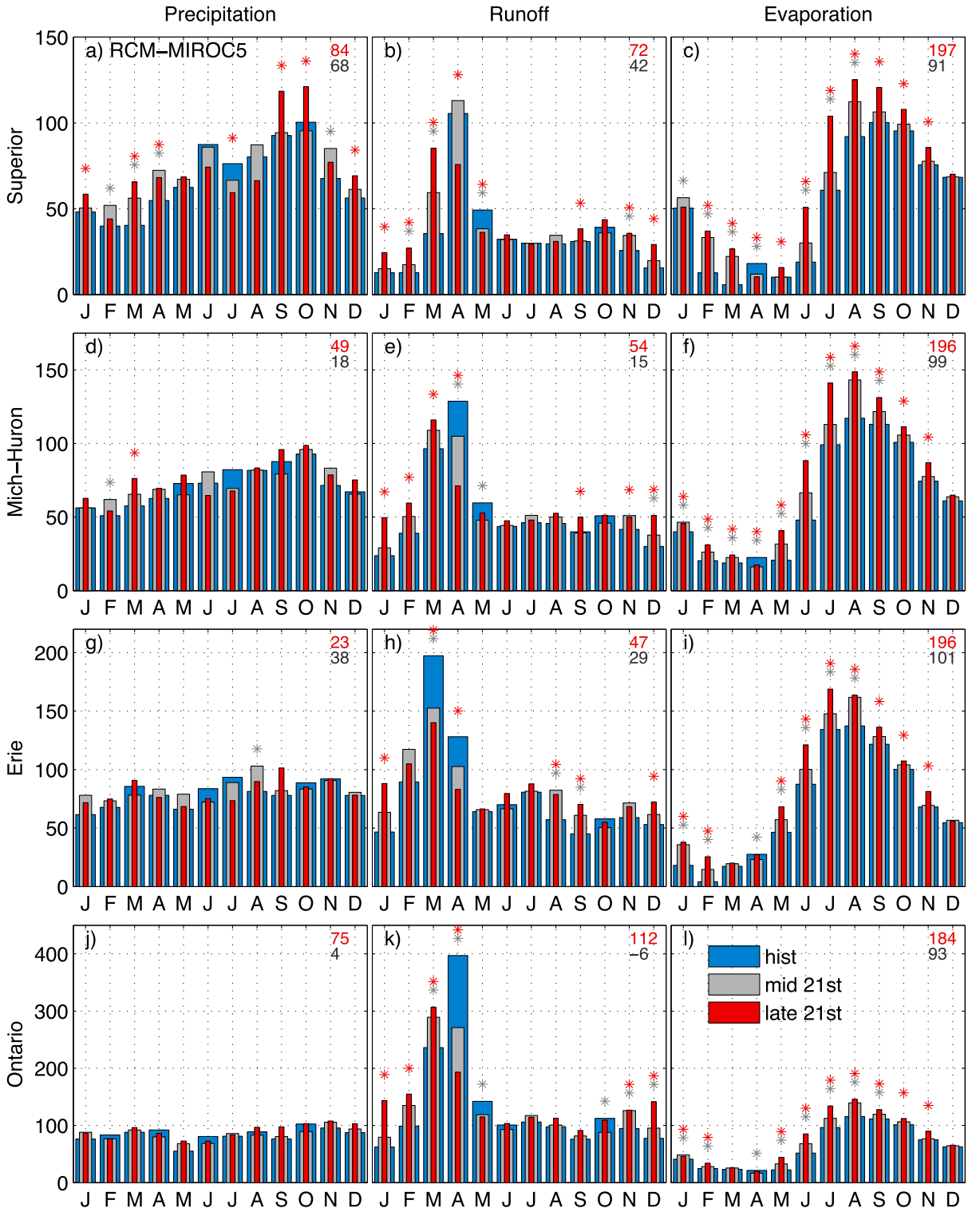

FIG. 9. Mean seasonal cycles of (a),(d),(g),(j) overlake precipitation, (b),(e),(h),(k) basin runoff, and (c),(f),(i),(l) lake evaporation, in millimeters of lake depth per month, for the late twentieth (blue; 1980–99), mid-twenty-first (gray; 2040–59), and late twenty-first (red; 2080–99) centuries from RCM-MIROC5. Results are shown for Lakes (a)–(c) Superior, (d)–(f) Michigan–Huron, (g)–(i) Erie, and (j)–(l) Ontario. Total annual-mean changes in each component for mid-twenty-first century and late twenty-first century (from late twentieth century) are denoted for each lake with black and red values, respectively. Significant changes ($p < 0.1$) by the mid- and late twenty-first century are indicated by gray and red asterisks, respectively.

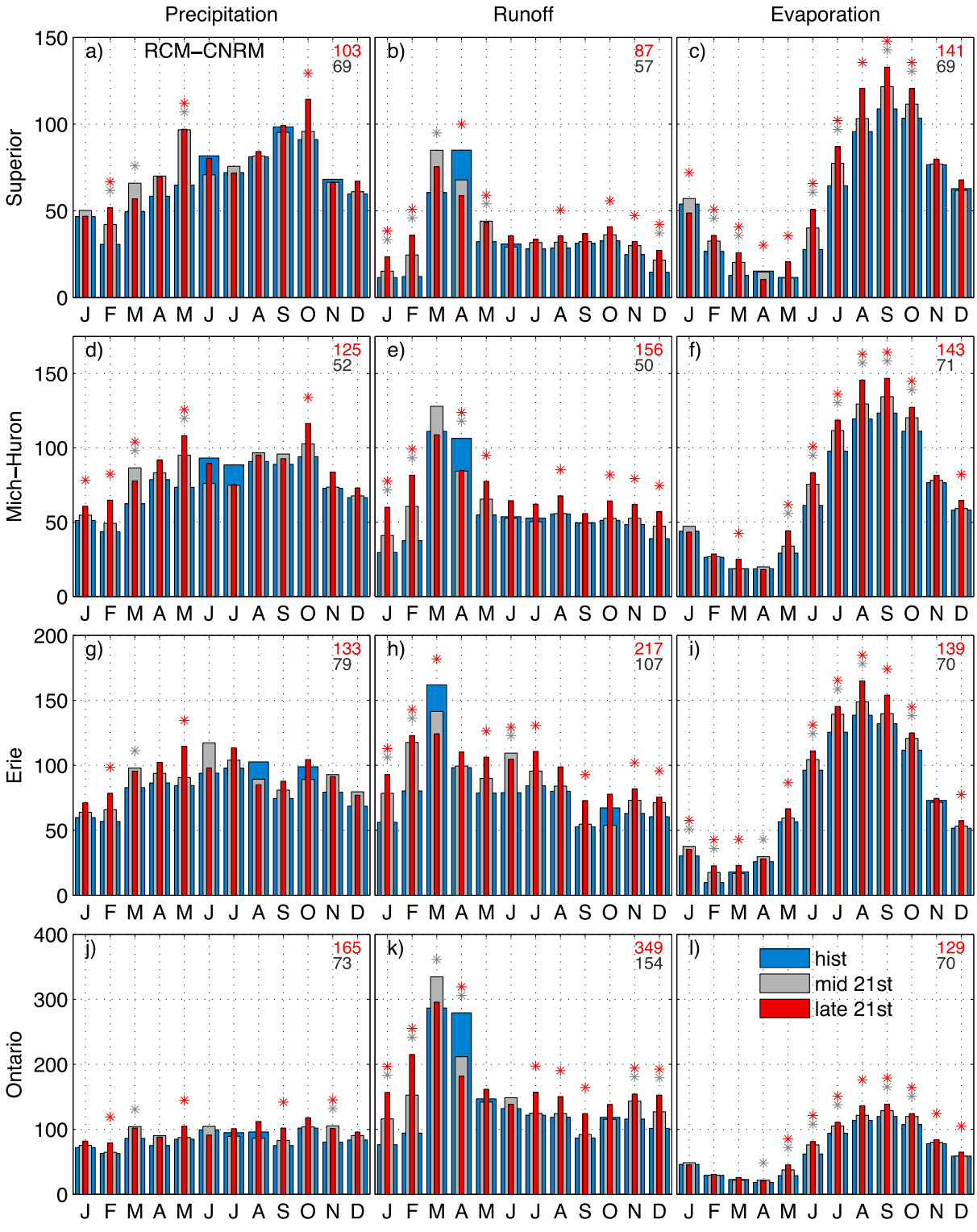

FIG. 10. As in Fig. 9, but for RCM-CNRM.

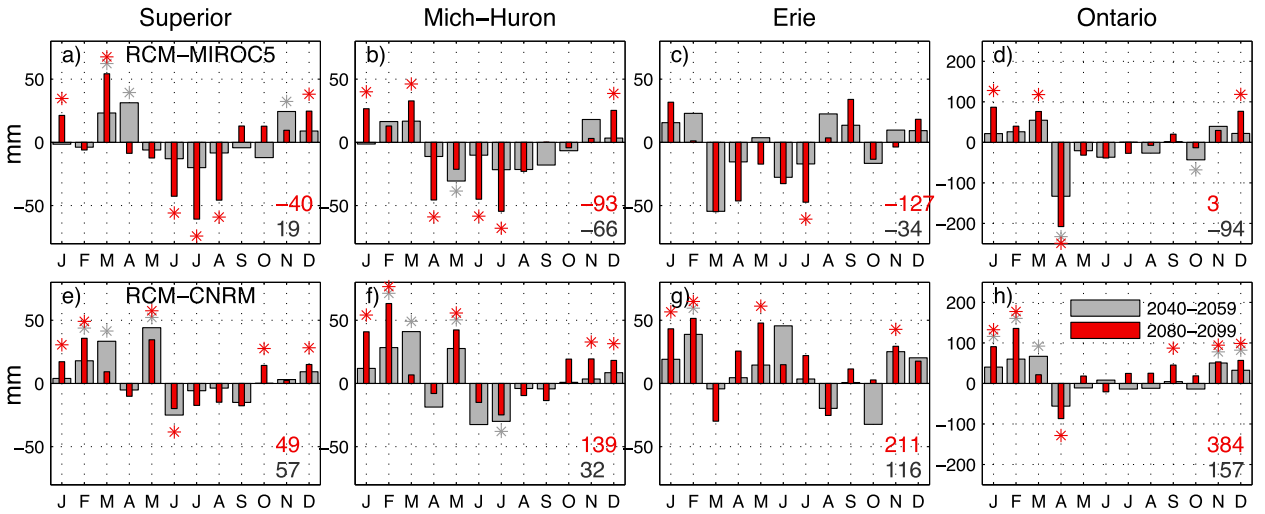

FIG. 11. Projected changes in the mean seasonal cycle of net basin water supply, in millimeters of lake depth, for Lakes (a),(e) Superior, (b),(f) Michigan–Huron, (c),(g) Erie, and (d),(h) Ontario from (a)–(d) RCM-MIROC5 and (e)–(h) RCM-CNRM by the mid-twenty-first century (gray; 2040–59) and late twenty-first century (red; 2080–99), compared to the late twentieth century (1980–99). Total annual changes are denoted with black and red values for the mid-twenty-first and late twenty-first century, relative to the late twentieth century. Significant changes ($p < 0.1$) by the mid- and late twenty-first century are indicated by gray and red asterisks, respectively.

by the late twenty-first century (Fig. 11); for both periods, all but one lake exhibit NBS declines. The NBS is projected to typically increase in December–March because of greater overlake precipitation and runoff and decrease in April–July because of reduced snowmelt-related runoff in middle-to-late spring and enhanced lake evaporation.

Within RCM-CNRM, the magnitudes of the annual changes in runoff and lake evaporation exceed that of overlake precipitation (Fig. 10). By the late twenty-first century, the increase in annual overlake precipitation ranges from +103 mm for Lake Superior to +165 mm for Lake Ontario. Similar to RCM-MIROC5, runoff generally increases during December–March because of greater precipitation and decreases during April because of a diminished snowpack. Both model configurations produce the greatest increase in lake evaporation during June–September. According to RCM-CNRM, projected NBS changes range from +32 mm for Lakes Michigan–Huron to +157 mm for Lake Ontario by the mid-twenty-first century and from +49 mm for Lake Superior to +384 mm for Lake Ontario by the late twenty-first century; for both time periods, every lake exhibits projected NBS increases, in contrast to RCM-MIROC5. The largest NBS increases are simulated for November–February and May because of greater precipitation over lakes and land. In summary, while both RCM-MIROC5 and RCM-CNRM simulate increases in annual lake evaporation, land evapotranspiration, and precipitation across the basin, their NBS projections are generally opposite of each other because of the relative magnitude of changes in each NBS component. In RCM-MIROC5, the large projected warming leads to dramatic increases in lake evaporation, which cannot be offset by modest increases in annual precipitation, leading to general declines in NBS. In contrast, RCM-CNRM produces more modest warming and increases in lake evaporation, which are dominated by substantial increases in regional precipitation (overlake precipitation plus runoff from land), leading to large NBS increases.

g. *Projected lake level changes*

The two model configurations suggest contrasting water level projections, with large increases in RCM-CNRM and moderate decreases in RCM-MIROC5 (Figs. 12 and 13). Projected NBS changes from RCM-CNRM lead to annual lake level changes ranging from +75 mm for Lake Superior to +180 mm for Lakes Michigan–Huron by the mid-twenty-first century and from +134 mm for Lake Superior to +420 mm for Lakes Michigan–Huron by the late twenty-first century. The seasonal cycle of projected lake level changes varies by lake, with the largest increases typically occurring in spring for Lakes Superior and Michigan–Huron and summer for Lake Erie. In contrast, projected NBS changes from RCM-MIROC5 suggest lake level declines, ranging from −24 mm for Lake Superior to −132 mm for Lakes Michigan–Huron by the mid-twenty-first century and from −97 mm for Lake Superior to −296 mm for Lakes Michigan–Huron by the late twenty-first century. With RCM-MIROC5, the largest declines in water levels occur in summer for Lake

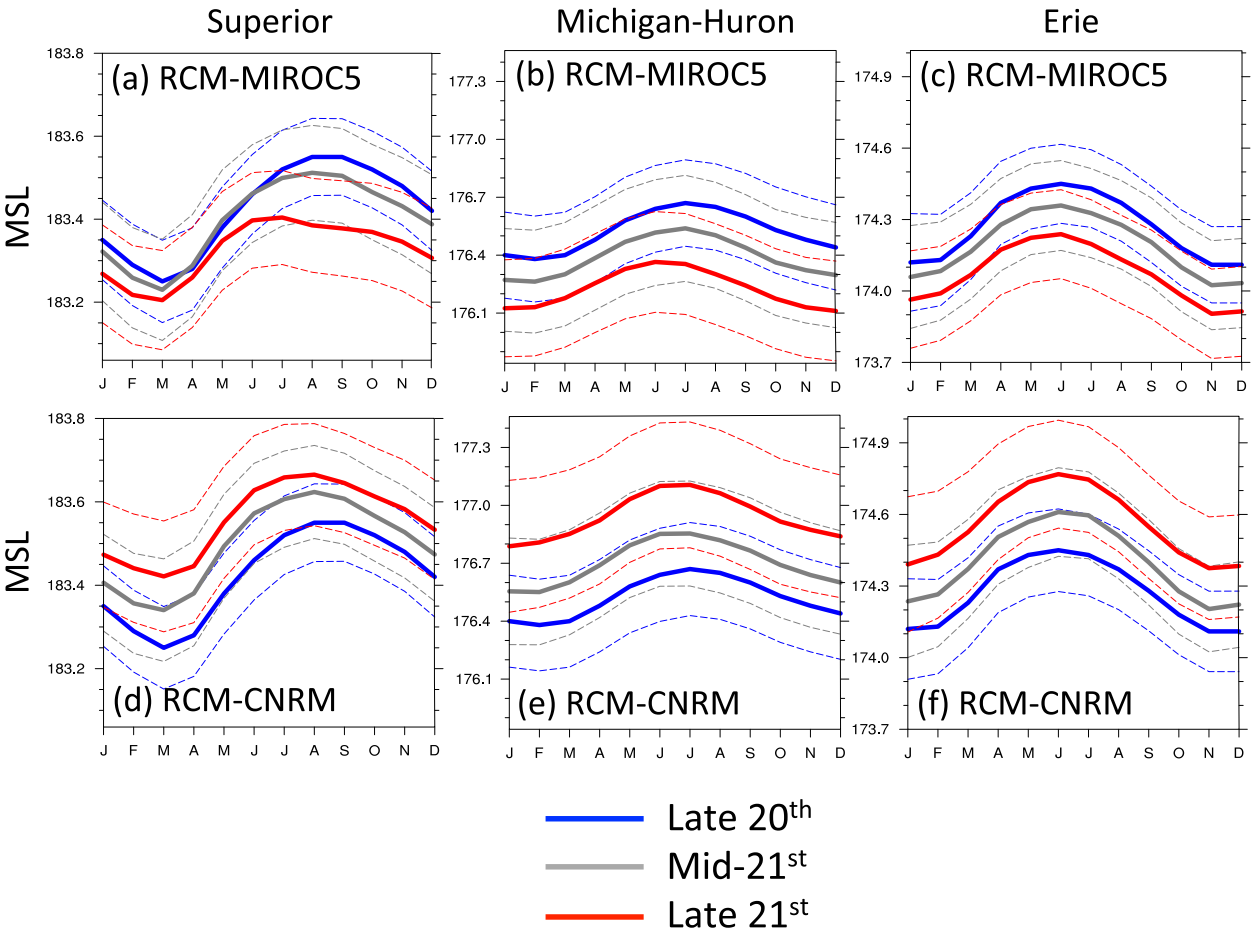

FIG. 12. Mean seasonal cycle of water levels (solid), in meters above sea level, on Lakes (a),(d) Superior, (b),(e) Michigan–Huron, and (c),(f) Erie for the late twentieth (blue), mid-twenty-first (gray), and late twenty-first (red) centuries, from (a)–(c) RCM-MIROC5 and (d)–(f) RCM-CNRM. Historical NBS estimates for 1948–2006 are obtained from the Great Lakes monthly hydrologic dataset. Projected lake levels are obtained by perturbing this historical-mean NBS with the mean and std dev in RCM-based projected changes in NBS (by 2040–59 or 2080–99) and then inputting these projected values of NBS into the NOAA GLERL channel model. Dashed lines indicate the interannual variability—namely, ±1 std dev in lake levels for each time period.

Erie, late summer–autumn for Lake Superior, and autumn for Lakes Michigan–Huron.

The chart (low water) datum is assigned as 183.2, 173.5, and 176.0 m above mean sea level for Lakes Superior, Erie, and Michigan–Huron, respectively. When lake levels fall below the chart datum, ships with standard 30-foot drafts must lighten their loads, leading to reduced efficiency. According to RCM-CNRM, the probability of water levels falling below the chart datum drops from 6.8% in the late twentieth century to 1.1% in the late twenty-first century for Lake Superior and from 1.7% in the late twentieth century to 0.1% in the late twenty-first century for Lakes Michigan–Huron. However, shipping concerns are greater with RCM-MIROC5 projections, which suggest an increase in this probability from 6.8% in the late twentieth century to 17.7% in the late twenty-first century for Lake Superior and from 1.1% in the late twentieth century to 20.1% in the late twenty-first century for Lakes Michigan–Huron.

4. Summary and discussion

The range of climate projections for the Great Lakes basin is assessed among 33 CMIP5 GCMs, leading to the selection of two GCMs with relatively high spatial resolution, reasonable performance in the study region, and contrasting climate projections. Simulations from CNRM-CM5 and MIROC5 for the late twentieth, mid-twenty-first, and late twenty-first centuries are dynamically downscaled using RegCM4, with 25-km grid spacing. The downscaling produces regional added value by reducing biases in the seasonal cycle of precipitation for CNRM and both air temperature and

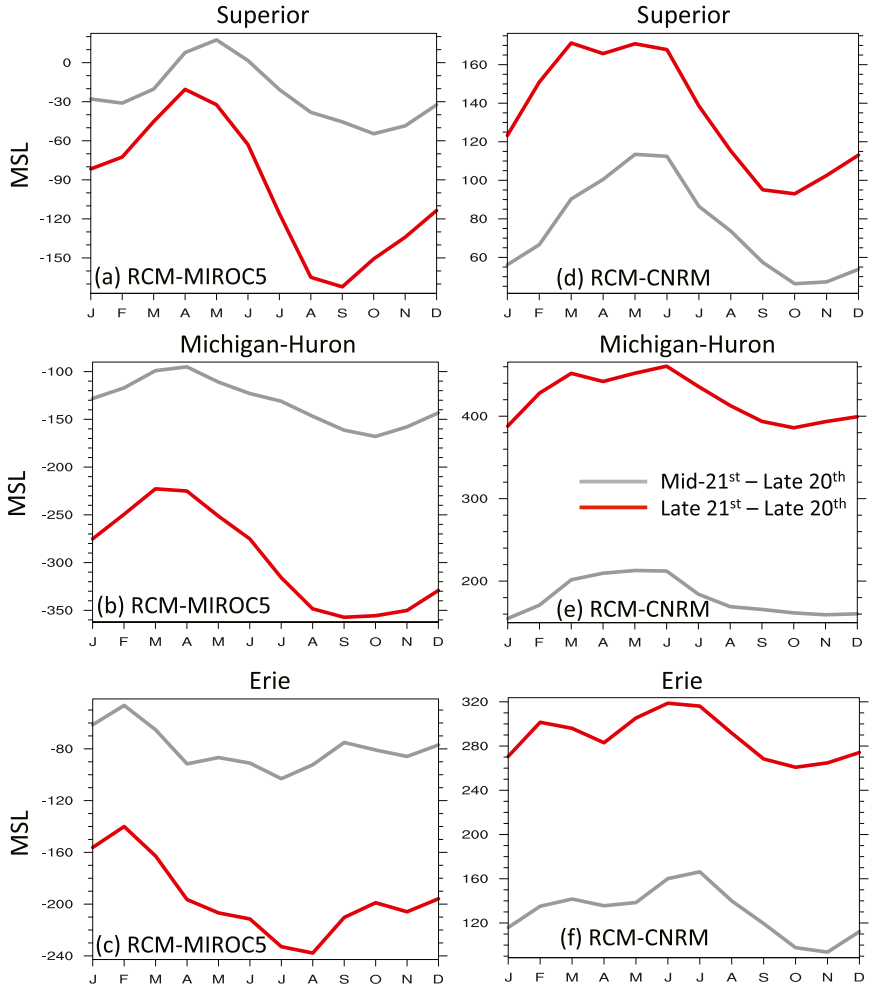

FIG. 13. Projected changes in water levels (mm) of Lakes (a),(d) Superior, (b),(e) Michigan–Huron, and (c),(f) Erie for the mid-twenty-first century (2040–59; gray) and late twenty-first century (2080–99; red), compared to the late twentieth century (1948–2006), from (a)–(c) RCM-MIROC5 and (d)–(f) RCM-CNRM.

precipitation for MIROC5. In general, RegCM4 simulates a reasonable seasonal cycle of LSTs, lake ice cover, and NBS, although with distinct biases that include warm summer biases in LSTs, excessive ice cover, and an early peak in lake evaporation.

Projected changes in the regional climate and NBS components are assessed for the Great Lakes basin. Both RCM-CNRM and RCM-MIROC5 simulate increases in annual temperature and precipitation by both the mid- and late twenty-first century, as do nearly all CMIP5 models, but the projected warming is notably greater in RCM-MIROC5, particularly in spring, and the projected increase in precipitation is greater in RCM-CNRM, particularly in late winter to spring. Both model configurations simulate increases in annual temperature and precipitation across the basin, yet their NBS projections are generally opposite of each other because of the relative magnitude of changes in each NBS component. The substantial warming in RCM-MIROC5 leads to greater lake evaporation, which cannot be offset by modest increases in annual precipitation, generally leading to NBS declines. RCM-CNRM, however, produces smaller increases in temperature and lake evaporation, which are overwhelmed by large increases in regional precipitation, leading to dramatic increases in NBS.

Lake level projections are developed for the mid- and late twenty-first century by driving a channel model with the historic NBS time series with RCM-based mean perturbations for the future periods. Consistent with NBS projections, large increases in water levels are projected by RCM-CNRM (e.g., +420 mm for Lakes Michigan–Huron by the late twenty-first century) while moderate decreases in water levels are projected by

RCM-MIROC5 (e.g., −296 mm for Lakes Michigan–Huron by the late twenty-first century). Lake level projections from RCM-MIROC5 suggest that the frequency of water levels on Lakes Superior and Michigan–Huron falling below the low water datum could nearly triple by the late twenty-first century, which is a serious shipping concern. The magnitudes of the mid-twenty-first-century projections in lake level changes are roughly twice as great as those produced by the RCM-based study of MacKay and Seglenieks (2013), although their study focuses on an earlier time period (2021–50 instead of 2040–59). The uncertainty in the sign of the projected changes in lake levels is consistent with previous studies in which there are competing influences due to changes in precipitation and evapotranspiration on land and water, producing different signs of lake level change (Lofgren et al. 2002; Angel and Kunkel 2010; and, using a conceptually different formulation, Lofgren et al. 2011). Precipitation and evapotranspiration generally increase in most models, but the relative magnitudes of these increases determine the sign of the NBS change.

Mean biases in RegCM4 have implications for the reliability of projected changes in lake conditions and regional climate. The model simulates a substantial positive bias in spring–summer LSTs, with lake stratification occurring too early. It is therefore possible that the projected rapid increase in springtime LSTs might be more likely to occur in summer instead. The model produces excessive historical lake ice cover, leading to much larger reductions in total ice cover than can be expected; this may exaggerate the projected impact on lake-effect snowfall (Notaro et al. 2015). Furthermore, the simulated seasonal cycle of lake evaporation peaks in early autumn rather than in early winter as observed. This puts the credibility of the projected increase in warm season evaporation into question.

Future studies on Great Lakes water level projections should ideally apply a nonhydrostatic RCM with higher spatial resolution, coupled to a three-dimensional lake model to represent the Great Lakes' circulation, in order to reduce biases in LSTs, ice cover, and stratification. An expanded pool of GCMs needs to be dynamically downscaled to capture the full spectrum of projected changes in NBS and lake levels, potentially on the order of 10–20 models (Alexandru et al. 2007; Meehl et al. 2009; Deser et al. 2012). Water resource managers need to prepare for the large interannual variability in lake levels already seen in the historical record, along with a potential expansion of the spread in lake levels to greater extremes.

Acknowledgments. This study was funded by NOAA Climate Change Data and Detection, NOAA/GLERL, and Michigan Department of Natural Resources (from Environmental Protection Agency funding). The authors appreciate the assistance of Drs. Graziano Guiliani, Nellie Elguindi, and Filippo Giorgi in improving the lake model and beneficial input from Drs. Andrew Gronewold and David Hart. Comments from three anonymous reviewers were extremely beneficial. We acknowledge the World Climate Research Programme's Working Group on Coupled Modelling, which is responsible for CMIP. We thank the modeling groups for producing and making available their output. For CMIP, the U.S. Department of Energy's Program for Climate Model Diagnosis and Intercomparison provides coordinating support and led development of software infrastructure in partnership with the Global Organization for Earth System Science Portals. Dr. Jennifer Adam provided the gauge-adjusted precipitation data. The National Science Foundation–sponsored NCAR Computational and Information Systems Laboratory provided computational resources.

REFERENCES

Ackerman, S. A., A. Heidinger, M. J. Foster, and B. Maddux, 2013: Satellite regional cloud climatology over the Great Lakes. *Remote Sens.*, **5**, 6223–6240, doi:10.3390/rs5126223.

Adam, J. C., and D. P. Lettenmaier, 2003: Adjustment of global gridded precipitation for systematic bias. *J. Geophys. Res.*, **108**, 4257, doi:10.1029/2002JD002499.

——, E. A. Clark, D. P. Lettenmaier, and E. F. Wood, 2006: Correction of global precipitation products for orographic effects. *J. Climate*, **19**, 15–38, doi:10.1175/JCLI3604.1.

Adams, R. M., and Coauthors, 1990: Global climate change and US agriculture. *Nature*, **345**, 219–224, doi:10.1038/345219a0.

Alexandru, A., R. de Elia, and R. Laprise, 2007: Internal variability in regional climate downscaling at the seasonal scale. *Mon. Wea. Rev.*, **135**, 3221–3238, doi:10.1175/MWR3456.1.

Amante, C., and B. W. Eakins, 2009: ETOPO1 1 arc-minute global relief model: Procedures, data sources, and analysis. NOAA Tech. Memo. NESDIS NGDC-24, 19 pp.

Angel, J. R., and S. A. Isard, 1998: The frequency and intensity of Great Lake cyclones. *J. Climate*, **11**, 61–71, doi:10.1175/1520-0442(1998)011<0061:TFAIOG>2.0.CO;2.

——, and K. E. Kunkel, 2010: The response of Great Lakes water levels to future climate scenarios with an emphasis on Lake Michigan-Huron. *J. Great Lakes Res.*, **36**, 51–58, doi:10.1016/j.jglr.2009.09.006.

Antic, S., R. Laprise, B. Denis, and R. de Elía, 2004: Testing the downscaling ability of a one-way nested regional climate model in regions of complex topography. *Climate Dyn.*, **23**, 473–493, doi:10.1007/s00382-004-0438-5.

Assel, R. A., 2003: An electronic atlas of Great Lakes ice cover winters: 1973–2002. [Available online at http://www.glerl.noaa.gov/data/ice/atlas/.]

——, 2005: Classification of annual Great Lakes ice cycles: Winters of 1973–2002. *J. Climate*, **18**, 4895–4905, doi:10.1175/JCLI3571.1.

——, S. Drobrot, and T. E. Croley, 2004: Improving 30-day Great Lakes ice cover outlooks. *J. Hydrometeor.*, **5**, 713–717, doi:10.1175/1525-7541(2004)005<0713:IDGLIC>2.0.CO;2.

Austin, J. A., and S. M. Colman, 2007: Lake Superior summer water temperatures are increasing more rapidly than regional air temperatures: A positive ice-albedo feedback. *Geophys. Res. Lett.*, **34**, L06604, doi:10.1029/2006GL029021.

Bates, G. T., S. W. Hostetler, and F. Giorgi, 1995: Two-year simulation of the Great Lakes region with a coupled modeling system. *Mon. Wea. Rev.*, **123**, 1505–1522, doi:10.1175/1520-0493(1995)123<1505:TYSOTG>2.0.CO;2.

Beltran, R., L. Botts, P. Brown, T. Clarke, D. Cowell, K. Fuller, and B. Krushelnicki, 1995: *The Great Lakes: An Environmental Atlas and Resource Book*. K. Fuller, H. Shear, and J. Wittig, Eds., Government of Canada and United States Environmental Protection Agency, 46 pp.

Bennington, V., M. Notaro, and K. Holman, 2014: Improving climate sensitivity of deep lakes within a regional climate model and its impact on simulated climate. *J. Climate*, **27**, 2886–2911, doi:10.1175/JCLI-D-13-00110.1.

Blanken, P. D., C. Spence, N. Hedstrom, and J. D. Lenters, 2011: Evaporation from Lake Superior: 1. Physical controls and processes. *J. Great Lakes Res.*, **37**, 707–716, doi:10.1016/j.jglr.2011.08.009.

Bodaly, R. A., J. W. M. Rudd, R. J. P. Fudge, and C. A. Kelly, 1993: Mercury concentrations in fish related to size of remote Canadian shield lakes. *Can. J. Fish. Aquat. Sci.*, **50**, 980–987, doi:10.1139/f93-113.

Botts, L., and B. Krushelnicki, 1988: *The Great Lakes: An Environmental Atlas and Resource Book*. U.S. Environmental Protection Agency, 46 pp.

Brown, R., W. Taylor, and R. A. Assel, 1993: Factors affecting the recruitment of lake whitefish in two areas of northern Lake Michigan. *J. Great Lakes Res.*, **19**, 418–428, doi:10.1016/S0380-1330(93)71229-0.

Bruce, J. P., 1984: Great Lakes levels and flows: Past and future. *J. Great Lakes Res.*, **10**, 126–134, doi:10.1016/S0380-1330(84)71819-3.

Burnett, A. W., M. E. Kirby, H. T. Mullins, and W. P. Patterson, 2003: Increasing Great Lake–effect snowfall during the twentieth century: A regional response to global warming? *J. Climate*, **16**, 3535–3542, doi:10.1175/1520-0442(2003)016<3535:IGLSDT>2.0.CO;2.

Changnon, S. A., 1993: Changes in climate and level of Lake Michigan: Shoreline impacts at Chicago. *Climatic Change*, **23**, 213–230, doi:10.1007/BF01091616.

Chao, P., 1999: Great Lakes water resources: Climate change impact analysis with transient GCM scenarios. *J. Amer. Water Resour. Assoc.*, **35**, 1499–1507, doi:10.1111/j.1752-1688.1999.tb04233.x.

Clites, A. H., and D. H. Lee, 1998: MIDLAKES: A coordinated hydrologic response model for the middle Great Lakes. NOAA Tech. Rep. ERL GLERL-109, 48 pp. [Available online at http://www.glerl.noaa.gov/ftp/publications/tech_reports/glerl-109/tm-109.pdf.]

Cohen, S. J., 1986: Impacts of CO_2-induced climatic change on water resources in the Great Lakes basin. *Climatic Change*, **8**, 135–153, doi:10.1007/BF00139751.

Croley, T. E., II, 1990: Laurentian Great Lakes double-CO_2 climate change hydrological impacts. *Climatic Change*, **17**, 27–47, doi:10.1007/BF00148999.

——, and T. S. Hunter, 1994: Great Lakes monthly hydrologic data. NOAA Tech. Memo. ERL GLERL-83, 13 pp. [Available online at http://www.glerl.noaa.gov/ftp/publications/tech_reports/glerl-083/report.pdf.]

——, F. H. Quinn, K. E. Kunkel, and S. A. Changnon, 1996: Climate transposition effects on the Great Lakes hydrological cycle. NOAA Tech. Memo. ERL GLERL-89, 107 pp. [Available online at http://ftp.glerl.noaa.gov/ftp/publications/tech_reports/glerl-089/tm-089.pdf.]

——, ——, ——, and ——, 1998: Great Lakes hydrology under transposed climates. *Climatic Change*, **38**, 405–433, doi:10.1023/A:1005344010723.

Crossman, E. J., and B. C. Cudmore, 1998: Biodiversity of the fishes of the Laurentian Great Lakes: A Great Lakes Fishery Commission project. *Ital. J. Zool.*, **65**, 357–361, doi:10.1080/11250009809386846.

DeMarchi, C., Q. Dai, M. E. Mello, and T. S. Hunter, 2010: Uncertainty quantification in the net basin supply of Lake Erie and Lake Michigan. *Proc. SimHydro 2010: Hydraulic Modeling and Uncertainty*, Sophia-Antipolis, France, Société Hydrotechnique de France.

Denis, B., R. Laprise, D. Caya, and J. Côté, 2002: Downscaling ability of one-way nested regional climate models: The Big-Brother Experiment. *Climate Dyn.*, **18**, 627–646, doi:10.1007/s00382-001-0201-0.

Desai, A. R., J. A. Austin, V. Bennington, and G. A. McKinley, 2009: Stronger winds over a large lake in response to weakening air-to-lake temperature gradient. *Nat. Geosci.*, **2**, 855–858, doi:10.1038/ngeo693.

Deser, C., A. Phillips, V. Bourdette, and H. Teng, 2012: Uncertainty in climate change projections: The role of internal variability. *Climate Dyn.*, **38**, 527–546, doi:10.1007/s00382-010-0977-x.

Dickinson, R. E., A. Henderson-Sellers, P. J. Kennedy, and M. Wilson, 1986: Biosphere-Atmosphere Transfer Scheme (BATS) for the NCAR Community Climate Model. NCAR Tech. Note NCAR/TN-275+STR, 69 pp. [Available online at http://nldr.library.ucar.edu/repository/assets/technotes/TECH-NOTE-000-000-000-527.pdf.]

——, ——, and ——, 1993: Biosphere-Atmosphere Transfer Scheme (BATS) version 1e as coupled to the NCAR Community Climate Model. NCAR Tech. Note NCAR/TN-387+STR, 72 pp. [Available online at http://nldr.library.ucar.edu/repository/assets/technotes/TECH-NOTE-000-000-000-198.pdf.]

Dominguez, F., J. Cañon, and J. Valdes, 2010: IPCC-AR4 climate simulations for the southwestern US: The importance of future ENSO projections. *Climatic Change*, **99**, 499–514, doi:10.1007/s10584-009-9672-5.

d'Orgeville, M., W. R. Peltier, A. R. Erier, and J. Gula, 2014: Climate change impacts on Great Lakes basin precipitation extremes. *J. Geophys. Res. Atmos.*, **119**, 10 799–10 812, doi:10.1002/2014JD021855.

Elguindi, N., and Coauthors, 2011: Regional Climatic Model RegCM user manual version 4.1. Abdus Salam International Centre for Theoretical Physics Rep., 32 pp.

Ellis, A. W., and J. J. Johnson, 2004: Hydroclimatic analysis of snowfall trends associated with the North American Great Lakes. *J. Hydrometeor.*, **5**, 471–486, doi:10.1175/1525-7541(2004)005<0471:HAOSTA>2.0.CO;2.

Ficke, A. D., C. A. Myrick, and L. J. Hansen, 2007: Potential impacts of global climate change on freshwater fisheries. *Rev. Fish Biol. Fish.*, **17**, 581–613, doi:10.1007/s11160-007-9059-5.

Fritsch, J. M., and C. F. Chappell, 1980: Numerical prediction of convectively driven mesoscale pressure systems. Part I: Convective parameterization. *J. Atmos. Sci.*, **37**, 1722–1733, doi:10.1175/1520-0469(1980)037<1722:NPOCDM>2.0.CO;2.

Fuller, K., and Coauthors, 1995: The Great Lakes: An environmental atlas and resource book. Government of Canada and U.S. Environmental Protection Agency Rep. 905-B-95-001, 51 pp.

Giorgi, F., and Coauthors, 2012: RegCM4: Model description and preliminary tests over multiple CORDEX domains. *Climate Res.*, **52**, 7–29, doi:10.3354/cr01018.

Grell, G. A., 1993: Prognostic evaluation of assumptions used by cumulus parameterizations. *Mon. Wea. Rev.*, **121**, 764–787, doi:10.1175/1520-0493(1993)121<0764:PEOAUB>2.0.CO;2.

——, J. Dudhia, and D. R. Stauffer, 1994: Description of the fifth-generation Penn State/NCAR Mesoscale Model (MM5). NCAR Tech. Note NCAR/TN-398+STR, 121 pp. [Available online at http://nldr.library.ucar.edu/repository/assets/technotes/TECH-NOTE-000-000-000-214.pdf.]

Grigal, D. F., 2002: Inputs and outputs of mercury from terrestrial watersheds: A review. *Environ. Rev.*, **10**, 1–39, doi:10.1139/a01-013.

Gronewold, A. D., V. Fortin, B. Lofgren, A. Clites, C. A. Stow, and F. Quinn, 2013: Coasts, water levels, and climate change: A Great Lakes perspective. *Climatic Change*, **120**, 697–711, doi:10.1007/s10584-013-0840-2.

Gula, J., and W. R. Peltier, 2012: Dynamical downscaling over the Great Lakes basin of North America using the WRF Regional Climate Model: The impact of the Great Lakes system on regional greenhouse warming. *J. Climate*, **25**, 7723–7742, doi:10.1175/JCLI-D-11-00388.1.

Hartmann, H. C., 1990: Climate change impacts on Laurentian Great Lakes levels. *Climatic Change*, **17**, 49–67, doi:10.1007/BF00149000.

Hayhoe, K., J. VanDorn, T. Croley II, N. Schlegal, and D. Wuebbles, 2010: Regional climate change projections for Chicago and the US Great Lakes. *J. Great Lakes Res.*, **36**, 7–21, doi:10.1016/j.jglr.2010.03.012.

Held, I. M., and B. J. Soden, 2006: Robust responses of the hydrological cycle to global warming. *J. Climate*, **19**, 5686–5699, doi:10.1175/JCLI3990.1.

Holman, K. D., A. D. Gronewold, M. Notaro, and A. Zarrin, 2012: Improving historical precipitation estimates over the Lake Superior basin. *Geophys. Res. Lett.*, **39**, L03405, doi:10.1029/2011GL050468.

Hostetler, S. W., 1991: Simulation of lake ice and its effect on the late-Pleistocene evaporation rate of Lake Lahontan. *Climate Dyn.*, **6**, 43–48, doi:10.1007/BF00210581.

——, and P. J. Bartlein, 1990: Simulation of lake evaporation with application to modeling lake level variations of Harney-Malheur Lake, Oregon. *Water Resour. Res.*, **26**, 2603–2612, doi:10.1029/WR026i010p02603.

——, G. T. Bates, and F. Giorgi, 1993: Interactive coupling of a lake thermal model with a regional climate model. *J. Geophys. Res.*, **98**, 5045–5057, doi:10.1029/92JD02843.

Kao, Y.-C., C. P. Madenjian, D. B. Bunnell, B. M. Lofgren, and M. Perroud, 2015: Temperature effects induced by climate change on the growth and consumption by salmonines in Lakes Michigan and Huron. *Environ. Biol. Fish.*, **98**, 1089–1104, doi:10.1007/s10641-014-0352-6.

Kiehl, J., J. Hack, G. Bonan, B. Boville, B. Breigleb, D. Williamson, and P. Rasch, 1996: Description of the NCAR Community Climate Model (CCM3). NCAR Tech. Note NCAR/TN-420+STR, 152 pp.

Kling, G. W., and Coauthors, 2003: Confronting climate change in the Great Lakes region: Impacts on our communities and ecosystems. Union of Concerned Scientists and Ecological Society of America Rep., 92 pp.

Kunkel, K., S. A. Changnon, T. E. Croley II, and F. H. Quinn, 1998: Transposed climates for study of water supply variability of the Laurentian Great Lakes. *Climatic Change*, **38**, 387–404, doi:10.1023/A:1005351026653.

——, K. Andsager, and D. R. Easterling, 1999: Long-term trends in extreme precipitation events over the conterminous United States and Canada. *J. Climate*, **12**, 2515–2527, doi:10.1175/1520-0442(1999)012<2515:LTTIEP>2.0.CO;2.

——, D. R. Easterling, K. Redmond, and K. Hubbard, 2003: Temporal variations of extreme precipitation events in the United States: 1895–2000. *Geophys. Res. Lett.*, **30**, 1900, doi:10.1029/2003GL018052.

——, L. Ensor, M. Palecki, D. Easterling, D. Robinson, K. G. Hubbard, and K. Redmond, 2009: A new look at lake-effect snowfall trends in the Laurentian Great Lakes using a temporally homogeneous data set. *J. Great Lakes Res.*, **35**, 23–29, doi:10.1016/j.jglr.2008.11.003.

——, and Coauthors, 2013: Regional climate trends and scenarios for the U.S. National Climate Assessment: Part 3. Climate of the Midwest U.S. NOAA Tech. Rep. NESDIS 142-3, 103 pp. [Available online at http://www.nesdis.noaa.gov/technical_reports/NOAA_NESDIS_Tech_Report_142-3-Climate_of_the_Midwest_U.S.pdf.]

Lindeberg, J. D., and G. M. Albercook, 2000: Climate change and Great Lakes shipping/boating. *Preparing for a Changing Climate: The Potential Consequences of Climate Variability and Change*, P. J. Sousounis and J. M. Bisanz, Eds., University of Michigan, 39–42. [Available online at www.geo.msu.edu/glra/PDF_files/Regional%20Summary/04F_WRES_F.boating.pdf.]

Linder, K., and M. Inglis, 1989: The potential effects of climate change on regional and national demands for electricity. EPRI Rep. 68-01-7033.

Lofgren, B. M., F. H. Quinn, A. H. Clites, R. A. Assel, A. J. Eberhardt, and C. L. Luukkonen, 2002: Evaluation of potential impacts on Great Lakes water resources based on climate scenarios of two GCMs. *J. Great Lakes Res.*, **28**, 537–554, doi:10.1016/S0380-1330(02)70604-7.

——, T. S. Hunter, and J. Wilbarger, 2011: Effects of using air temperature as a proxy for potential evapotranspiration in climate change scenarios of Great Lakes basin hydrology. *J. Great Lakes Res.*, **37**, 744–752, doi:10.1016/j.jglr.2011.09.006.

MacKay, M., and F. Seglenieks, 2013: On the simulation of Laurentian Great Lakes water levels under projections of global climate change. *Climatic Change*, **117**, 55–67, doi:10.1007/s10584-012-0560-z.

Mackey, S., 2012: Great Lakes nearshore and coastal systems. U.S. National Climate Assessment Midwest Tech. Input Rep., 14 pp. [Available online at http://glisa.umich.edu/media/files/NCA/MTIT_Coastal.pdf.]

Magnuson, J., and Coauthors, 1995: Region 1—Laurentian Great Lakes and Precambrian shield. *Proc. Symp. Report: Regional Assessment of Freshwater Ecosystems and Climate Change in North America*, Leesburg, VA, U.S. Environmental Protection Agency and U.S. Geological Survey, 3–4. [Available online at http://www.aslo.org/meetings/Freshwater_Ecosystems_Symposium.pdf.]

Mallard, M. S., C. G. Nolte, O. R. Bullock, T. L. Spero, and J. Gula, 2014: Using a coupled lake model with WRF for dynamical downscaling. *J. Geophys. Res. Atmos.*, **119**, 7193–7208, doi:10.1002/2014JD021785.

——, ——, T. L. Spero, O. R. Bullock, K. Alapaty, J. A. Herwehe, J. Gula, and J. H. Bowden, 2015: Technical challenges and

solutions in representing lakes when using WRF in downscaling applications. *Geosci. Model Dev.*, **8**, 1085–1096, doi:10.5194/gmd-8-1085-2015.

Marchand, D., M. Sanderson, D. Howe, and C. Alpaugh, 1988: Climatic change and Great Lakes levels: The impact on shipping. *Climatic Change*, **12**, 107–133, doi:10.1007/BF00138935.

Martynov, A., L. Sushama, and R. Laprise, 2010: Simulation of temperate freezing lakes by one-dimensional lake models: Performance assessment for interactive coupling with regional climate models. *Boreal Environ. Res.*, **15**, 143–164.

——, ——, ——, K. Winger, and B. Dugas, 2012: Interactive lakes in the Canadian Regional Climate Model, version 5: The role of lakes in the regional climate of North America. *Tellus*, **64A**, 16226, doi:10.3402/tellusa.v64i0.16226.

Maurer, E. P., A. W. Wood, J. C. Adam, D. P. Lettenmaier, and B. Nijssen, 2002: A long-term hydrologically based dataset of land surface fluxes and states for the conterminous United States. *J. Climate*, **15**, 3237–3251, doi:10.1175/1520-0442(2002)015<3237:ALTHBD>2.0.CO;2.

Meehl, G. A., and Coauthors, 2009: Decadal prediction: Can it be skillful? *Bull. Amer. Meteor. Soc.*, **90**, 1467–1485, doi:10.1175/2009BAMS2778.1.

Millerd, F., 2011: The potential impact of climate change on Great Lakes international shipping. *Climatic Change*, **104**, 629–652, doi:10.1007/s10584-010-9872-z.

Mortsch, L., and F. H. Quinn, 1996: Climate change scenarios for Great Lakes basin ecosystem studies. *Limnol. Oceanogr.*, **41**, 903–911, doi:10.4319/lo.1996.41.5.0903.

——, H. Hengeveld, M. Lister, L. Wenger, B. Lofgren, F. Quinn, and M. Slivitzky, 2000: Climate change impacts on the hydrology of the Great Lakes-St. Lawrence system. *Can. Water Resour. J.*, **25**, 153–179, doi:10.4296/cwrj2502153.

Moss, R. H., and Coauthors, 2010: The next generation of scenarios for climate change research and assessment. *Nature*, **463**, 747–756, doi:10.1038/nature08823.

Music, B., A. Frigon, B. Lofgren, R. Turcotte, and J.-F. Cyr, 2015: Present and future Laurentian Great Lakes hydroclimatic conditions as simulated by regional climate models with an emphasis on Lake Michigan-Huron. *Climatic Change*, **130**, 603–618, doi:10.1007/s10584-015-1348-8.

Niimi, A. J., 1982: Economic and environmental issues of the proposed extension of the winter navigation season and improvements on the Great Lakes-St. Lawrence Seaway system. *J. Great Lakes Res.*, **8**, 532–549, doi:10.1016/S0380-1330(82)71991-4.

Notaro, M., K. Holman, A. Zarrin, S. Vavrus, and V. Bennington, 2013a: Influence of the Laurentian Great Lakes on regional climate. *J. Climate*, **26**, 789–804, doi:10.1175/JCLI-D-12-00140.1.

——, A. Zarrin, S. Vavrus, and V. Bennington, 2013b: Simulation of heavy lake-effect snowstorms across the Great Lakes basin by RegCM4: Synoptic climatology and variability. *Mon. Wea. Rev.*, **141**, 1990–2014, doi:10.1175/MWR-D-11-00369.1.

——, V. Bennington, and S. Vavrus, 2015: Dynamically downscaled projections of lake-effect snow in the Great Lakes basin. *J. Climate*, **28**, 1661–1684, doi:10.1175/JCLI-D-14-00467.1.

Pal, J. S., E. E. Small, and E. A. B. Eltahir, 2000: Simulation of regional-scale water and energy budgets: Representation of subgrid cloud and precipitation processes within RegCM. *J. Geophys. Res.*, **105**, 29 579–29 594, doi:10.1029/2000JD900415.

Pall, P., M. Allen, and D. Stone, 2007: Testing the Clausius–Clapeyron constraint on changes in extreme precipitation under CO_2 warming. *Climate Dyn.*, **28**, 351–363, doi:10.1007/s00382-006-0180-2.

Patterson, J. C., and P. F. Hamblin, 1988: Thermal simulation of a lake with winter ice cover. *Limnol. Oceanogr.*, **33**, 323–338, doi:10.4319/lo.1988.33.3.0323.

Pryor, S. C., D. Scavia, C. Downer, M. Gaden, L. Iverson, R. Nordstrom, J. Patz, and G. P. Robertson, 2014: Midwest. *Climate Change Impacts in the United States: The Third National Climate Assessment*, J. M. Melillo, T. C. Richmond, and G. W. Yohe, Eds., U.S. Global Change Research Program, 418–440, doi:10.7930/J0J1012N.

Quinn, F. H., 1978: Hydrologic response model of the North American Great Lakes. *J. Hydrol.*, **37**, 295–307, doi:10.1016/0022-1694(78)90021-5.

Reifen, C., and R. Toumi, 2009: Climate projections: Past performance no guarantee of future skill? *Geophys. Res. Lett.*, **36**, L13704, doi:10.1029/2009GL038082.

Reutter, J. M., and Coauthors, 2011: Lake Erie nutrient loading and harmful algal blooms: Research findings and management implications. Lake Erie Millennium Network Synthesis TeamFinal Rep., 17 pp. [Available online at http://www.ohioseagrant.osu.edu/_documents/publications/TS/TS-060%20June2011LakeErieNutrientLoadingAndHABSfinal.pdf.]

Schwab, D., G. Leshkevich, and G. Muhr, 1992: Satellite measurements of surface water temperature in the Great Lakes: Great Lakes Coastwatch. *J. Great Lakes Res.*, **18**, 247–258, doi:10.1016/S0380-1330(92)71292-1.

Smith, J. B., 1991: The potential impacts of climate change on the Great Lakes. *Bull. Amer. Meteor. Soc.*, **72**, 21–28, doi:10.1175/1520-0477(1991)072<0021:TPIOCC>2.0.CO;2.

Steiner, A. L., J. S. Pal, F. Giorgi, R. E. Dickinson, and W. L. Chameides, 2005: The coupling of the Common Land Model (CLM0) to a regional climate model (RegCM). *Theor. Appl. Climatol.*, **82**, 225–243, doi:10.1007/s00704-005-0132-5.

——, ——, S. A. Rauscher, J. L. Bell, N. S. Diffenbaugh, A. Boone, L. C. Sloan, and F. Giorgi, 2009: Land surface coupling in regional climate simulations of the West African monsoon. *Climate Dyn.*, **33**, 869–892, doi:10.1007/s00382-009-0543-6.

Stephens, G. L., and T. D. Ellis, 2008: Controls of global-mean precipitation increases in global warming GCM experiments. *J. Climate*, **21**, 6141–6155, doi:10.1175/2008JCLI2144.1.

Takata, K., S. Emori, and T. Watanabe, 2003: Development of the minimal advanced treatments of surface interaction and runoff. *Global Planet. Change*, **38**, 209–222, doi:10.1016/S0921-8181(03)00030-4.

Taylor, K. E., R. J. Stouffer, and G. A. Meehl, 2012: An overview of CMIP5 and the experiment design. *Bull. Amer. Meteor. Soc.*, **93**, 485–498, doi:10.1175/BAMS-D-11-00094.1.

Vaccaro, L., and J. Read, 2011: Vital to our nation's economy: Great Lakes jobs. Michigan Sea Grant 2011 Rep., 7 pp. [Available online at http://www.fws.gov/glri/documents/2011GreatLakesJobsReport.pdf.]

Vanderploeg, H. A., S. J. Bolsenga, G. L. Fahnenstiel, J. R. Liebig, and W. S. Gardner, 1992: Plankton ecology in an ice-covered bay of Lake Michigan: Utilization of a winter phytoplankton bloom by reproducing copepods. *Hydrobiologia*, **243**, 175–183, doi:10.1007/BF00007033.

van Vuuren, D., and Coauthors, 2011: The representative concentration pathways: An overview. *Climatic Change*, **109**, 5–31, doi:10.1007/s10584-011-0157-y.

Voldoire, A., and Coauthors, 2013: The CNRM-CM5.1 global climate model: Description and basic evaluation. *Climate Dyn.*, **40**, 2091–2121, doi:10.1007/s00382-011-1259-y.

Wang, J., X. Bai, H. Hu, A. Clites, M. Colton, and B. Lofgren, 2012: Temporal and spatial variability of Great Lakes ice cover, 1973–2010. *J. Climate*, **25**, 1318–1329, doi:10.1175/2011JCLI4066.1.

Watanabe, M., and Coauthors, 2010: Improved climate simulation by MIROC5: Mean states, variability, and climate sensitivity. *J. Climate*, **23**, 6312–6335, doi:10.1175/2010JCLI3679.1.

Willmott, C. J., and K. Matsuura, 2000: Terrestrial air temperature and precipitation: Monthly and annual time series (1950-1996), version 1.01. Center for Climatic Research, accessed 1 Apr 2008. [Available online at http://climate.geog.udel.edu/~climate/html_pages/download.html.]

Yediler, A., and J. Jacobs, 1995: Synergistic effects of temperature; oxygen and water flow on the accumulation and tissue distribution of mercury in carp (*Cyprinus carpio L.*). *Chemosphere*, **31**, 4437–4453, doi:10.1016/0045-6535(95)00324-2.